An Investigation of

TRANSFORMATION CHARACTERISTICS OF THREE URANIUM BASE ALLOYS

Final Report

Conducted by

THE DEPARTMENT OF METALLURGY
CASE INSTITUTE OF TECHNOLOGY

Technical Report AMRA CR 63-02/1(F)
Final Report
Contract DA-33-019-ORD-3630
Cleveland Procurement District, U. S. Army
AMC Code 5566. 12. 58900
D/A Project 5N12-15-030
U. S. Army Materials Research Agency
Watertown 72, Mass.

Prepared by:

P. E. Repas
Graduate Assistant

R. H. Goodenow
Graduate Assistant

R. F. Hehemann
Professor

January, 1963

The findings in this report are not to be construed as an official Department of the Army position.

ASTIA AVAILABILITY NOTICE

Qualified requesters may obtain copies of this report from ASTIA.

DISPOSITION INSTRUCTIONS

Destroy; do not return.

ABSTRACT

The present investigation has been directed toward two main objectives. These were: (1) to develop TTT diagrams for several uranium base alloys, and (2) to develop metallographic techniques suitable for the identification of phases, intermetallic compounds and nonmetallic constituents in these and several other alloys. Accordingly, the following report will be presented in two parts dealing separately with each of these topics.

TTT diagrams are presented and transformation kinetics are described for five alloys: (1) U-10%Mo, (2) U-8%Mo, (3) U-8%Mo-1/2%Ti, (4) U-8%Mo-1%Ti , and (5) U-2%Mo-2%Nb-2%Zr-1/2%Ti. Metallographic, dilatometric, hardness and x-ray techniques were utilized in establishing the TTT diagrams. Sensitivity and limitations of each technique are discussed.

Metallographic techniques have been perfected for the uranium base alloys for nearly all conditions of heat treatment. Certain low temperature transformation structures and the identification of nonmetallic inclusions have not been completely resolved. Metallographic structures of the specimens submitted by U. S A my Materials Research Agency are interpreted where possible in terms of the established TTT diagrams.

PART I: TTT INVESTIGATIONS

LITERATURE REVIEW

Numerous studies of the alloying behavior and transformation characteristics of uranium base alloys have appeared in the unclassified literature during the past fifteen years. A complete compilation of equilibrium diagrams for binary and ternary uranium alloys was prepared by Rough and Bauer in 1958 (1) All binary phases, certain ternary phases and most intermetallic compounds of interest here may be obtained from this source. Ternary and more complex phases and intermetallics have received much less attention and in many instances their existence and identification remain to be established. Ternary systems of some interest here, in which equilibrium diagrams have been reported include U-Mo-Ti (2) U-Mo-Zr (3) U-Mo-Nb (1, 4) and U-Nb-Zr (5).

Transformation kinetics of certain uranium base alloys have been studied fairly extensively, although in most instances only in an exploratory manner. Only in the most recent investigations have detailed studies been performed, all of which point out the inadequacies of the early investigations. Because of the extensive nature of this subject only those investigations pertinent to the present study will be reviewed.

Uranium-molybdenum and uranium-niobium have been the most widely studied systems, mainly because the metastable gamma phase alloys in these systems have been of interest as possible fuel materials. The binary U-Mo system has been studied quite extensively and today many of

the aspects of the transformation behavior in this system are well known. However, significant differences still exist between various investigations.

Quenching studies (6, 7) as well as the results of other investigations to be mentioned later, have indicated that rapid cooling from the high temperature gamma phase region produces several structures depending on alloy content. For alloys with less than about 4%Mo* a distorted alpha structure is obtained, variously designated as α_a, α'_β, and α''_β (8) depending on metallographic appearance. From 4 to 5.4% Mo a tetragonal phase forms on quenching, designated γ_o, while with alloys having from 5.4 to approximately 20%, the limit of solid solubility of molybdenum in gamma uranium, the gamma phase may be retained at room temperature by quenching, or even slow cooling, from the gamma region. One report however (7), indicates that the quenched structure is partially ordered in alloys having from 5.5 to 9.2%Mo.

Lehmann (9) has studied transformations in 0.5 to 4% Mo alloys. Of interest is the transformation behavior of alloys with greater than 1% Mo held in the $\alpha + \gamma$ region. Lehmann found the characteristic lamellar structure found in alloys with higher molybdenum contents but until this time not reported for alloys with less than about 5%Mo.

The majority of the remaining investigations have centered about the alloys in which the gamma phase may be retained at room temperature. The earliest studies on 10-15%Mo alloys (10) and 5.4-12%Mo alloys (11)

---

*All percentages will be given in terms of weight percent.

resulted in very incomplete TTT diagrams usually indicating only the times for the initiation of transformation. Comparing metallographic observations with hardness and resistivity measurements, Van Thyne and McPherson (11) found that metallography was most sensitive for detection of incipient transformation in 5.4 and 8%Mo alloys at high transformation temperature where a lamellar transformation product was observed. However, inconsistent results were found in these alloys below about 450°C (842°F) and at all transformation temperatures in the case of 10 and 12%Mo alloys. In these latter instances no transformation products could be observed metallographically. Mikhailoff (12) has presented a rather complete description of transformation kinetics in 6 and 10%Mo alloys and seems to be the only one who has examined the low temperature transformation behavior in any detail. He found the low temperature reactions to be associated with an initial precipitation of α in a U-6%Mo alloy and with an initial precipitation of γ' in a U-10%Mo alloy. At higher temperatures the characteristic lamellar or cellular reaction was observed to proceed as $\gamma \rightarrow \alpha+\gamma \rightarrow \alpha+\gamma+\gamma' \rightarrow \alpha+\gamma'$ for the U-6%Mo alloy and as $\gamma \rightarrow \alpha+\gamma'$ for the U-10%Mo alloy. In the former alloy the initial γ lamellae are not enriched sufficiently to produce the ordered γ' phase. For intermediate temperatures a mixture of the two transformation mechanisms was encountered.

Other transformation studies on this system have centered about the gamma prime phase. These investigations (13-18) have verified that the gamma to gamma prime transformation is an ordering reaction

which transforms the bcc gamma structure into an ordered tetragonal structure. Holland (16) and Kramer and Rhodes (17, 18) have recently reported an intermediate, metastable transformation product in U-14%Mo and U-16%Mo alloys and have identified it as the alpha phase of uranium.

Uranium-columbium alloys have been studied (19, 20) and their transformation behavior is similar to that of U-Mo alloys, at least in composition ranges where the gamma phase may be retained at room temperature.

Ternary and more complex systems have been examined to a quite limited extent although here again the U-Mo and U-Nb systems have been studied with various ternary and quaternary additions, especially the U-Mo-Nb system (4, 19, 21) where small additions of niobium (1-4%) have been found to retard transformations in gamma phase U-Mo base alloys. The effects on the gamma phase stability of ternary and quaternary additions of Cr, Mo, Nb, Ru, V, and Zr to U-Mo, U-Nb, and U-Zr base alloys is discussed in the paper by Storhok et al (22) In general, Mo, Nb and Ru stabilized the gamma phase, Zr additions lowered its stability, and V and Cr had little effect.

The influence of titanium additions on the transformation behavior of U-Mo alloys, of especial interest here, has not been reported in the literature. The solubility of titanium in both the alpha and gamma prime phases of the U-Mo system is reported to be quite small (2, 23), probably on the order of 0.1%. By itself, titanium has not proved to be an effective

gamma stabilizer, for even with alloying additions as high as 30%, the gamma phase can not be retained at room temperature (23).

EXPERIMENTAL PROCEDURE

MATERIALS

The alloys employed in this study were prepared by Army Materials Research Agency, Watertown, Massachusetts. The identification and nominal analysis of these alloys are listed below:

Alloy No.	Nominal Analysis - wt% Mo	Ti	Cb	Zr
E 139	10			
E 101	8			
E 88	8	1		
E 107	8	1/2		
E 105	2	1/2	2	2

SPECIMEN PREPARATION

Metallographic, dilatometer and x-ray specimens (to be described later) were machined from the appropriate alloys, cleaned, individually wrapped in molybdenum foil, and sealed in Vycor capsules under a vacuum of 0.5 -1x10^{-4} mm Hg. To ensure a uniform initial condition for the alloys to be used in the TTT investigations, the following homogenization treatment was found satisfactory:

1. Solution heat treat the encapsulated specimens for four hours at 980°C (1796°F) and water quench without breaking the capsules.

2. Reheat to 900°C (1650°F) for one hour prior to transferring the specimens to the desired transformation temperature.

Both 900°C (1650°F) and 980°C (1795°F) are well within the single phase gamma regions for the alloys under consideration.

METALLOGRAPHIC, HARDNESS and X-RAY SPECIMENS

After receiving the thermal treatment described above, the specimens were transferred directly to the desired isothermal holding temperature. Conventional salt pots were used with a temperature control of $\pm$ 3°C. After the desired holding time the capsules were quenched to room temperature by breaking them under water.

Knoop hardness readings, using a 500 gm load, were taken on the metallographic specimens after they were prepared metallographically (see Part II). The specimens were approximately 1/8" x 1/8" x 3/16".

X-ray samples (1/8" round x 1/2" long) having received the desired isothermal treatment, were machined on one end to 0.035" and electrolytically polished to .010" in the standard electropolishing solution (see Part II) at an open circuit potential of 18-20 volts D. C. Since the gamma prime phase reverts to gamma on cold working (11) the effects of machining after heat treatment were examined. Several specimens were electrolytical ly polished from 1/8" to 0.010" and showed no differences from those normally machined to 0.035" and then polished to 0.010". Debye patterns were obtained using nickel filtered copper radiation and a camera of 114.6 mm diameter. In order to ensure additional precision, no

filter was used for determining the lattice parameters of the as-quenched retained gamma phase alloys. For all cubic phases a standard $\cos^2 \theta$ extrapolation was used to determine the lattice parameters.

DILATOMETRY

Dilatometry was utilized for determining critical temperatures and for following isothermal transformations in the alloys under investigation. For isothermal transformations, dilatometry was found most useful with the U-2%Mo-2%Nb-2%Zr-1/2%Ti alloy while in most instances with the other alloys, where transformation times were excessively long, only the start of transformation could be detected near the nose of the TTT curve.

The dilatometer consisted of two concentric quartz rods to which the specimen was attached. The inner rod was free to move against a linear variable differential transformer. The signal from the LVDT was amplified and transmitted to a Leeds and Northrup recorder.

Specimens of size 1/16" x 5/32" x 1", with 3/4" between two holes used for attachment to the quartz rods, were initially encapsulated, heated to 980°C (1795°F) for four hours and water quenched. In this condition the specimens were mechanically and electrolytically polished to remove any surface film, etched in concentrated nitric acid, and immediately copper plated. Plating was accomplished in an acid bath of copper sulfate at 90°C - 120°C and 50 APS for 1 to 2 hours which resulted in a plate thickness of about 0.001 inch. Prior to testing, the

plated specimens were coated with a commercial high temperature protective coating. *

The specimen, attached to the quartz rods, was heated to 900°C (1650°F) for 15 minutes in a tube furnace containing a partial helium atmosphere. At the end of this time the assembly was transferred to either another tube furnace or to a salt pot, the latter being used for the U-2%Mo-2%Nb-2%Zr-1/2%Ti alloy at low temperatures where transformation occurred rapidly and it was desired to attain temperature as quickly as possible. The dilation was recorded during the heating, cooling and holding periods.

For the critical temperature studies, those dilatometer specimens which had been isothermally transformed at 500°C (930°F) were at the completion of the isothermal test, immediately heated in approximately 10°C intervals, held at each temperature from one-half to one hour for equilibrium to be attained, and the dilation recorded. For the U-10%Mo alloy, excessively long transformation times prevented this procedure from being followed. Instead, a dilatometer specimen (not plated) was encapsulated, heated to 900°C (1650°F) for one hour, isothermally transformed at 500°C (930°F) for 500 hours and water quenched. The specimen was then cleaned and plated, attached to the dilatometer, heated to 500°C and then heated slowly in 10°C intervals. Due to the slow reaction kinetics of this alloy, it is unlikely that any errors were introduced by this method.

---

*Trade name: Markal Protection Coating Manufactured by Markal Company, 3052 West Carroll Avenue, Chicago, Illinois.

SPECIAL TECHNIQUES

For the U-2%Mo-2%Nb-2%Zr-1/2%Ti alloy, isothermal holding times of less than six minutes were studied by utilizing copper plated specimens which were not encapsulated, in order that the time required to reach temperature be a minimum. Samples were prepared in a similar manner to the dilatometer specimens. After copper plating, the specimens were heated to 900°C (1650°F) for one hour in a tube furnace and then transferred directly to a salt pot at the desired temperature.

RESULTS

Metallographic and x-ray data will be presented in connection with each alloy. In general, metallography proved effective for studying high temperature transformations where either a cellular or Widmanstatten transformation product could be observed, but not at low temperatures where no discrete precipitate could be detected.

Hardness measurements of the isothermally transformed metallographic specimens are presented in Figs. 1-5. Where the cellular transformation product was encountered, a weighted average was taken of the hardnesses of the transformed and untransformed areas based on a visual estimate of the extent of transformation. At low transformation temperatures no distinct hard and soft areas were detected and a general hardening of the entire matrix occurred. Similar curves for a more limited number of temperatures based on dilatometry are presented in Figs. 6 and 7.

In all instances transformation from γ was accompanied by contraction except for the complex alloy (U-2%Mo-2%Nb-2%Zr-1/2%Ti) isothermally transformed at 625°C (1155°F) where an expansion occurred.

Critical temperatures, determined dilatometrically, are summarized in Table I and typical dilation curves are presented in Figs. 8, 9 and 26. A comparison of linear coefficients of thermal expansion in the low temperature and single phase gamma ranges with the data of Saller et al (24) on similar alloy compositions shows good agreement (Table II) indicating that the copper plating had little effect even quantitatively on the expansion characteristics of the alloys under investigation.

DISCUSSION

A comparison of results based on metallography with hardness, dilatometric and x-ray data indicates quite consistent results. As expected, the latter three modes of determining transformation kinetics, usually being insensitive to small percentages of decomposition, proved in many instances to be inferior to metallography for the detection of incipient transformation. However, metallography was unsatisfactory at low temperatures for all alloys. Hardness data appear most reliable at these lower temperatures for detecting the start of transformation since the hardening occurs throughout the matrix and thus the problem of soft and hard regions is not encountered.

BINARY U-8%Mo and U-10%Mo ALLOYS

The high temperature γ phase of these alloys may be retained at room temperature by quenching or even by comparatively slow cooling. The retained γ phase of the 10% Mo alloy had a lattice parameter of $3.415 \pm .001$ Å, comparable to an accepted value for a U-10%Mo alloy of 3.4139 Å (25). The lattice parameter of retained γ in the 8%Mo alloy was 3.426 Å which agrees well with the accepted value of 3.4251 Å (25).

The microstructure of the quenched 10%Mo alloy is illustrated in Fig. 10 and is typical of that of both the 8% and 10% Mo alloys. The small amounts of dispersed inclusions are believed to be primarily oxides (see Part II).

Time-Temperature-Transformation diagrams for the 8%Mo and 10%Mo alloys are presented in Figs. 11 and 12. While the TTT diagram for the 10%Mo alloy has been determined in detail, less attention was devoted to the 8%Mo alloy so only the most essential features of its transformation characteristics are illustrated in Fig. 12.

The critical temperatures for these alloys are listed in Table I. The lower critical, or eutectoid temperature for both alloys was approximately 573°C (1064°F). Published values for this temperature vary from 560°C (1040°F) to 575°C (1066°F) although the latter is the more widely accepted value and agrees well with that observed in this study.

As illustrated in the TTT diagrams, the subcritical decomposition

of gamma in these U-Mo alloys is relatively complex and involves several different reaction mechanisms. These are represented by separate "C" curves in the TTT diagrams and, for convenience of discussion, will be divided into high temperature and low temperature reactions. The high temperature reactions have received considerable attention in the literature (11, 15, 19) while it has only recently been recognized that fundamentally different reaction mechanisms operate at lower temperatures (12).

High Temperature Reactions

The decomposition of γ at temperatures above approximately 450°C (842°F) takes place primarily, but not exclusively, by the cellular mechanism which has been described frequently in the literature (11, 12, 15, 19). In addition, alpha uranium also precipitates in a poorly defined Widmanstatten form as will be demonstrated shortly.

CELLULAR REACTION

Decomposition of both the 8% Mo and 10% Mo alloys is initiated by the cellular reaction at temperatures above approximately 375°C (705°F). The appearance of this product at 550°C (1022°F) in the 10% Mo alloy is illustrated in Fig. 12*. Decomposition has not started in 24 hours (Fig. 13a) and the lamellar nature of the cellular transformation

---

*Comparison of Figs. 10 and 13a reveals that a fine precipitate, delineating sub grain boundaries in the matrix, appears prior to the cellular product. This precipitate appeared after very short aging times and may represent a dislocation decoration by segregation of interstitial solutes.

product is clearly evident in Fig. 13b. This transformation is nucleated primarily at γ grain boundaries and, to a lesser extent at inclusions. The reaction gradually consumes the entire γ phase and the interlamellar spacing of the cellular product decreases rapidly with decreasing reaction temperature.

The cellular transformation mechanism also occurs above the eutectoid temperature (25) as is demonstrated in Fig. 14 for the 8% Mo alloy transformed at 585°C (1085°F). The formation of the pearlitic rather than a Widmanstatten precipitation of α uranium at a temperature above the eutectoid is somewhat unexpected and cannot be rationalized fully at present. Presumably, this must be viewed as another example of the discontinuous precipitation observed in many age hardening systems (26).

Clearly, the cells formed at temperatures above the eutectoid consist of alternate lamellae of α uranium and enriched γ whose composition is dictated by the $\alpha + \gamma$ solvus line. Below the eutectoid temperature, the cells also consist initially of α uranium and enriched γ rather than γ' as would be expected for normal eutectoid reactions. This has been reported previously (12, 15) and was confirmed in the present investigation by x-ray diffraction studies. Lattice parameter measurements demonstrated that the composition of the enriched gamma phase corresponded to the metastable extrapolation of the $\alpha + \gamma / \gamma$ solvus line so that the cellular reaction both above and below the eutectoid occurs initially by the same mechanism.

At temperatures below the eutectoid, the enriched γ phase in the cellular structure eventually orders to form γ'. This aspect of the transformation can not be revealed metallographically but can be detected by the appearance of γ' diffraction lines in the x-ray pattern. The initiation of γ' is indicated on the TTT diagram by a dashed line. This transformation occurs within the lamellar structure and the compositional readjustments required for the formation of γ' from the enriched γ presumably are accomplished by sidewise growth of the α lamellae.

WIDMANSTATTEN ALPHA

Precipitation of α uranium in a poorly defined Widmanstatten form competes with the cellular reaction in the high temperature range. The development of this structure in the 8%Mo alloy transformed at 450° C (842° F) is illustrated in Fig. 15. These α platelets nucleate at the substructure precipitate and eventually completely envelope the subgrain boundaries. Apparently, these precipitates serve as nucleation sites for the α uranium. Donze and Cabane (15) have interpreted the substructure markings as α particles at all reaction times; however, it was observed in the present investigation that these markings also develop at temperatures above the solvus (in the E107 alloy) which would suggest that this interpretation is oversimplified. Donze and Cabane (15) also have observed that the gammatizing temperature exerts a strong influence on the tendency to decompose with the Widmanstatten rather than the cellular morphology.

Specifically, lower gammatizing temperatures increase the extent of decomposition by the Widmanstatten mode which is consistent with the interpretation that the substructure precipitate merely serves as nucleation sites for the subsequent precipitation of α uranium.

The extent of decomposition to the Widmanstatten morphology increased significantly with reduction of the transformation temperature below the critical and was significantly greater in the 8%Mo than in the 10%Mo alloy. Thus, it appears that the Widmanstatten mechanism requires a substantially higher driving force for its activation than does the cellular mechanism. The Widmanstatten precipitates also offer little impedance to the cellular reaction which was observed to grow around and envelope the platelets without causing them to redissolve. It is apparent that the cellular reaction in these alloys is not induced by matrix recrystallization as has been proposed for this decomposition mechanism in many age hardening systems.

LOW TEMPERATURE DECOMPOSITION

No metallographic indications of transformation could be observed at reaction temperatures below approximately 375°C (705°F). Nevertheless, substantial hardening (Figs. 1 to 4) accompanied isothermal holding in this temperature range.

X-ray diffraction studies revealed that decomposition at these low temperatures was initiated by the formation of ordered γ', in agreement with the data of Mikhailoff (12). Diffraction patterns of the 10%Mo

alloy transformed at 400°C are compared in Fig. 16 with patterns from the as quenched γ structure and that of a specimen transformed completely to α plus γ' at 500°C.

An important difference exists between the diffraction patterns associated with samples transformed in the high temperature and the low temperature ranges. The diffraction lines of the retained γ phase are spotty (Fig. 16a) due to the large γ grain size. Transformation to the cellular structure at 500°C (932°F) results in smooth and continuous diffraction lines of the α and γ' phases (Fig. 16b) indicating the absence of discrete lattice relationships between these phases and the surrounding γ matrix. This is a characteristic of cellular reactions. The transformation products that form at low temperatures bear a discrete lattice relationship with the parent phase as demonstrated by spotty diffraction lines of the α and γ' phases (Figs. 16c and 16d).

Transformation in the low temperature range is initiated by the formation of oriented γ' as evidenced by the absence of α diffraction lines in the x-ray pattern (Fig. 16c). This transformation results in uniform hardening of the γ grains and consequently occurs more or less uniformly throughout the entire grain. The α phase forms, also with a lattice relationship to the γ phase, on continued isothermal transformation (Fig. 16d), however, this stage of the decomposition sequence also cannot be revealed metallographically. Unfortunately, the lack of metallographic evidence hampers further interpretation of the reaction

mechanism. The development of streaks, connecting γ and γ' diffraction spots in x-ray diffraction patterns suggests that a single crystal x-ray diffraction study would help considerably in the interpretation of this important transformation sequence.

At intermediate temperatures in the range 375°C (707°F) to 450°C (842°F) decomposition occurs by both the high temperature, cellular reaction, and by the low temperature decomposition mechanism. Transformation is initiated by the cellular reaction; however, growth of this product is arrested as the matrix is hardened by the low temperature transformation. The two reactions occur at different rates so that the extent of decomposition by the cellular mode decreases rapidly as the reaction temperature is lowered from 450°C (842°F) to 375°C (707°F). For example, in the 10% molybdenum alloy, approximately 80% transformation to the cellular product occurs at 450°C (Fig. 17). At 400°C, (Fig. 18) only about 5% of the γ matrix transformed by the cellular reaction before this transformation was arrested by conversion of the matrix to the low temperature products. No cellular products were observed at temperatures below 375°C (707°F).

Substructure delineation also occurred at temperatures in the range 350°C (662°F) to 400°C (752°F) (Fig. 19) but was not detected at lower temperatures. The significance of these structures is not yet fully understood since α diffraction lines first appear in the diffraction pattern long after such structures are well developed metallographically.

The influence of molybdenum on transformation kinetics is revealed by comparison of the TTT curves in Figs. 11 and 12. The same basic reactions occur at all temperatures in the two alloys; however, the decomposition rates are increased considerably by reduction of the molybdenum content from 10 to 8%.

TERNARY U-Mo-Ti-ALLOYS

The addition of 1/2% or 1%Ti to the binary U-8%Mo alloy exerts only minor effects on the transformation characteristics. TTT diagrams for these alloys are presented in Figs. 20 and 21 where it is apparent that the same high and low temperature reactions observed in binary U-Mo alloys also are operative in these ternary alloys. Titanium additions up to 1% results in , at most, a very slight increase in the rates of these decomposition processes but introduce an additional reaction at high temperatures - precipitation of the ε phase of the Mo-Ti system. *

Titanium additions influence significantly the critical temperatures of these U-Mo alloys (Table I). While the eutectoid temperature is raised by only 10°C by the addition of 1% titanium, a three phase $\alpha + \gamma + \varepsilon$ region occurs above the eutectoid temperature rather than the two phase $\alpha + \gamma$ region of the binary U-Mo system. The titanium addition raises significantly the upper temperature limit for the existence of the α phase. On slow heating α disappears before ε so that a two phase $\gamma + \varepsilon$ region appears to separate the $\alpha + \gamma + \varepsilon$ and the single phase γ region.

---

*This is the BCC solid solution of Mo and Ti and contains some U in solid solution in these alloys (2).

The microstructures of the 1/2% and 1%Ti alloys quenched from 900°C (1652°F) are compared in Fig. 22. While the 1/2% titanium alloy is single phase, the 1% alloy exhibits segregated areas where particles of a second phase are present. * These are undissolved particles of the ε phase. The number and distribution of these particles was not influenced significantly by solution treating for times up to 10 hours at 1100°C (2012°F). Thus, their presence appears to reflect alloy segregation and the upper critical temperature has been placed at 656°C (1215°F) on the basis of the dilatometric study (Fig. 9).

The most significant effect of the titanium addition on the transformation characteristics of the U-8%Mo alloy was the addition of a new reaction, precipitation of the ε phase, in the high temperature range. Metallographic evidence for precipitation of ε is obtained most easily in the two phase γ + ε region (Fig. 23). Between the eutectoid temperature and 450°C traces of the ε phase were evident in x-ray diffraction patterns and this phase was not observed to form at temperatures of 400°C and below. The ε phase nucleates primarily at γ grain boundaries and to a lesser extent at special sites within the grains.

Formation of ε appeared to take place independently of the cellular reaction characterisitic of the binary U-Mo alloys. Comparison

---

*This phase may be extracted electrolytically and exhibits a BCC structure with a lattice parameter of 3.17Å, close to that of tungsten. Our earlier identification of these particles as tungsten contaminants was incorrect.

of Figs. 2 to 4 demonstrates that the addition of 1/2 or 1% titanium to the 8%Mo base increases very slightly the rate of the cellular reaction which may reflect the tendency of titanium to stabilize the α phase as indicated by the elevation of the critical temperatures. The undissolved ε particles in the 1% titanium alloy did not serve as nuclei for the cellular reaction which usually nucleated on gamma grain boundaries in areas free of the ε phase.

THE U-2%Mo-2%Nb-2%Zr-1/2%Ti ALLOY

The TTT diagram for the U-2%Mo-2%Nb-2%Zr-1/2%Ti (E105) alloy is presented in Fig. 24. Transformation occurs by different mechanisms at high and at low reaction temperatures in this alloy just as in the binary U-Mo and ternary U-Mo-Ti alloys; however, the reactions in the E105 alloy differ considerably from those observed in the binary or ternary alloys. In contrast to the U-Mo and the U-Mo-Ti alloys, the γ phase could not be retained in the E105 alloy by water quenching to room temperature. The quenched structure exhibited very weak, spotty and diffuse α and γ diffraction lines corresponding to the formation of a distorted α within the original γ matrix. This transformation appears to take place martensitically* and corresponds to the distorted martensitic alpha observed in the other dilute U-Mo alloys (6-9). While

---

*Relief markings developed on the surface of previously polished samples.

the microstructure associated with this martensitic alpha could not be revealed clearly by conventional metallographic techniques (Fig. 25a), examination under polarized light of previously anodized samples produced the structure illustrated in Fig. 25b.

The dilation curve employed for the determination of the critical temperatures is illustrated in Fig. 26. In spite of the complex composition of this alloy, evidence could be found for only two critical temperatures corresponding to the γ / α + γ solvus line and the eutectoid temperature. No evidence for the Mo-Ti ε phase or the UZr_2 intermetallic compound was obtained.

Within the α + γ region 600°C-647°C, transformation of the metastable γ matrix proceeds by the nucleation and growth of α platelets having a Widmanstatten morphology. These individual platelets were distributed uniformly throughout the grains with a slight tendency to cluster at grain boundaries (Fig. 27). The existence of a lattice relationship between the α and γ phases, expected from the Widmanstatten morphology was confirmed by x-ray studies on samples which had been transformed for sufficiently long times so that sufficient α had formed to enrich and stabilize the remaining γ matrix when quenched to room temperature. The spotty α and γ lines indicated a lattice relationship between the two phases. No other phases were detected even after holding times of 500 hours at 625°C.

At temperatures between approximately 475°C (887°F) and the

eutectoid temperature 600°C (1112°F) transformation also occurred by the nucleation of acicular α although at these temperatures the α platelets were clustered in a fashion similar to that in the U-Mo and U-Mo-Ti alloys.(Fig. 28) Small amounts of a lamellar structure also formed at some grain boundaries. As expected from its relatively high Ti + Zr content and relatively low Mo+Nb content, the rate of transformation was extremely rapid in this alloy compared with that of the 8 to 10% Mo alloys. The formation of γ' * required long transformation times (300-400 hours at 500°C) and no phases other than α, γ and γ' were detected.

The ability to detect transformation metallographically disappeared abruptly at transformation temperatures between 470°C (879°F) and 475°C (888°F). However, samples treated at temperatures below 470°C increased substantially in hardness. Tentatively, it is assumed that the M_s temperature for the formation of martensitic alpha lies in this temperature range and consequently the M_s temperature has been placed at 472°C (881°F) on Fig. 24.

Isothermal transformation below M_s takes place at extremely high rates as evidenced by rapid hardening (Fig. 5). Comparison of Figs. 1 to 5 reveals that the E105 alloy attains the highest hardness of any of the alloys employed in this investigation. The mechanical behavior of these alloys deserve careful study and correlation with the varied transformation

---

*Although the term γ' will be used in connection with the E105 alloy, this phase is not identical to that found in the U-Mo system. Slight differences in lattice parameters were observed; however, it was not possible to analyze these further.

characteristics revealed in the present investigation.

X-ray diffraction studies reveal that transformation at temperatures below M_s involves tempering of martensitic α as well as decomposition of the primary γ phase. Conversion of the distorted martensitic α to equilibrium alpha was observed by displacements of the α diffraction lines to positions corresponding to those of equilibrium alpha. In addition, precipitation of a BCC phase with a lattice parameter of $3.102 \pm .002$ Å and the ordered γ' phase were observed. The BCC phase appeared very early in the reaction sequence while γ' lines became evident only after extremely long transformation times. A positive identification of the BCC phase has not been accomplished and the complex reactions occurring in this alloy require much further study before they will be fully understood.

Part II METALLOGRAPHY

In the past, the metallography of uranium has been approached mainly from the standpoint of developing suitable techniques for pure alpha uranium. Extreme care was necessary to eliminate such problems as surface flow and twinning, while the retention of inclusions presented further difficulties. However, these drawbacks encountered with the metal uranium are seldom found in uranium base alloys, especially alloys in which the gamma phase is stabilized to room temperature. Numerous investigators have utilized similar metallographic procedures for both unalloyed and alloyed uranium, superior results being obtained for the latter. Excellent review articles covering the metallography of uranium have appeared during the past several years (27, 28) so that an extensive bibliography is unwarranted here.

The identification of nonmetallic inclusions in uranium has been developed concurrently with the metallographic studies (27, 28) but has been hampered somewhat because of the isomorphous nature of UO, UN and UC. Although many of the obstacles here have been surmounted (29-31,) positive identification still presents certain difficulties, especially where alloys have only a small number of dispersed inclusions. The best method of identification seems to be the electrodeposition technique of Kehl et al (31) based on the time to electrodeposit copper on the inclusions and the nature of the deposit. The process, however, is tedious and could not be utilized for routine metallographic examinations .

MATERIALS

The alloys studied in this phase of the investigation included:

Alloy No.	Percent Alloy Content					
	Mo	Ti	Nb	Zr	V	Fe
E 88	8	1	---	---	---	---
E96	6	1	---	---	---	---
E101	8	--	---	---	---	---
E103	8	1/2	---	---	---	05
E105	2	1/2	2	2	---	---
E106	2	1/2	2	---	2	---
E107	8	1/2	---	---	---	---
E108	8	1/2	---	---	---	---
E111	8	1/2	---	---	---	---
E119	7	1/2	---	---	---	---
E120	71/2	1/2	---	---	---	---
E139	10	---	---	---	---	---
RL52	2	1/2	2	2	---	---
RL55	2	1/2	2	---	2	---

METALLOGRAPHIC TECHNIQUES

The standard polishing procedure presented in the Appendix is applicable to all alloys investigated and has been utilized in preparing all specimens whose photomicrographs appear in this report. As may be evidenced by these photomicrographs, surface preparation was quite satisfactory.

Etching techniques are somewhat sensitive to alloy composition and even more so to heat treatment. The general rules to be followed are discussed in the Appendix. Cellular and Widmanstatten phases, associated with high transformation temperatures, are easily revealed, while at lower

temperatures it usually was not possible to reveal the course of transformation metallographically.

The complex E105 alloy deserves special attention in certain respects and is treated separately in the last section of the Appendix.

IDENTIFICATION OF METALLIC PHASES

The metastable γ phase is readily identified by its unreactive nature when exposed to the standard polishing and etching procedures. The photomicrographs presented in Part I (Figs. 10, 22) adequately illustrate the appearance of this phase. As mentioned earlier the as-quenched structure of the complex E105 alloy also exhibits a similar etching behavior (Fig. 25a) although polarized light and x-ray diffraction reveal the presence of martensitic alpha (Fig. 25b). Thus, in studying alloys with complex compositions or low levels of alloy additions it is desirable to initially employ polarized light and x-ray studies, in addition to standard metallographic examination, in order to positively identify the γ phase.

The equilibrium α phase, characterized by its high chemically reactive nature, is easily detected when appearing either as a product of the cellular reaction or as discrete or grouped platelets displaying a Widmanstatten morphology. These various forms of α have all been described and illustrated in Part I.

The last, truly metallic phase encountered in the present alloys was the ε phase. This phase when present in small amounts, appears

similar to inclusions but may usually be distinguished from the latter by distribution and shape differences. The ε phase is usually concentrated at grain boundaries (Fig. 23) and does not display the flat-sided geometrical shapes associated with oxide, nitride, carbide and hydride inclusions. Further, this phase is relatively unattacked by etching.

INTERMETALLIC AND NONMETALLIC PHASE IDENTIFICATION

The only intermetallic compound identified in the alloys under investigation was the γ' phase (U_2Mo). The presence of this phase could only be revealed by x-ray diffraction patterns. It was not possible to reveal metallographically the domain pattern associated with γ' in alloys containing 12% to 16%Mo. (8, 16, 17).

Nonmetallic phase identification was hampered by the small quantities of inclusions present in most alloys and, by the reactive nature of these inclusions with various solutions utilized for attempted electrolytic extraction. This was particularly true of the flat sided, geometrically shaped inclusions which may be seen in many of the photomicrographs presented here.

Various anodizing and etching procedures were attempted in order to correlate color or chemical behavior with these inclusions, but unsuccessful results were obtained. Based on the results of previous investigations where alloys with deliberately added impurities were studied, the shape of these particles suggest that they are in all probability mainly

UO. The isomorphous nature of the UN and UC with UO also suggests that these inclusions are actually some mixture of the three and that the chemical formula should be written as U (O, N, C). Further, polarized light examination proved these inclusions to be cubic, in agreement with their interpretation is U (O, N, C) which is face centered cubic.

The E106 and RL55 alloys (U-2%Mo-2%Nb-2%V-1/2%Ti) exhibited large numbers of dispersed, elongated inclusions (Fig. 29). X-ray diffraction patterns of various samples of these alloys showed in addition to γ and α lines a weak set of what appeared to be a BCC phase with a lattice parameter of 3.099 ± 0.002 Å. Subsequent diffraction patterns of these particles alone, electrolytically extracted from the γ matrix of the water quenched sample, * showed additional lines indicating a more complex crystal structure. On the basis of d values and relative intensities these inclusions were identified tentatively as (V, Ti)N, primarily with vanadium. However a more positive identification of this phase would be desirable.

The lattice parameter of the above inclusions, based on a BCC structure, is comparable to the BCC phase found in the complex E105 alloy. However, the analogy is not complete. The latter alloy contains no vanadium, and the BCC phase appears only on isothermal transformation below the

---

*The standard electropolishing solution described in the Appendix was utilized for extraction. A voltage range of 30-40 volts D. C. was used and the bulk specimen partially immersed in the electrolyte for a time of about one hour. The solution was decanted and the residue washed thoroughly. Examination of the residue microscopically clearly revealed it to be the same elongated particles observed in the bulk specimen.

M_s and could not be observed metallographically. No intermetallics or ternary phases have been reported in the literature which could account for these phases. *

Finally, the E103 alloy (U-8%Mo-1/2%Ti-.05%Fe) contained a moderate number of dispersed inclusions which were quite chemically reactive and could not be extracted electrolytically. It is believed that these inclusions are associated with the iron alloying addition.

PHASE IDENTIFICATION IN HEAT TREATED ALLOYS RECEIVED FROM U. S. ARMY MATERIALS RESEARCH AGENCY

Phase identification in these specimens was accomplished mainly through utilization of the metallographic techniques and observations established in conjunction with the TTT studies. X-ray diffraction and hardness measurements were used to confirm metallographic identification or to positively establish the phases in any uncertain cases. Many of the photomicrographs for these alloys have been included in previous reports (Monthly Status Reports 10 and 11) so that only typical microstructure will be included here. Table III lists the structural state of each of the samples.

All of the alloys except E105 retained the γ phase upon quenching

---

*The possibility that the "BCC" phases in the E105 and E106 alloys represent terminal solutions analogous to the Mo-Ti ϵ phase observed in the E88 and E107 alloys or modifications of the U Zr_2 or U_2Ti phases requires clarification.

to room temperature. In this connection, it is significant to compare the behavior of the E105 and E106 alloys which differ only in that 2%Zr in the E105 alloy has been replaced by 2%V in the E106 alloy. The latter alloy (E106) retains the γ phase upon quenching while the E105 alloy transforms martensitically to distorted α as has been demonstrated in Part I. This difference in behavior may be attributed to the stabilizing influence of Zr on the α phase while V, like Nb and Mo, stabilizes the γ phase.

The alloys which retain γ upon quenching may be expected to decompose during subcritical aging in essentially the same way as during direct isothermal transformation. Thus, TTT curves, where available, can be employed with confidence in the interpretation of structures in all alloys except E105.

At an aging temperature of 204°C (400°F) and in the as quenched and as extruded conditions, all of the alloys with high molybdenum contents showed only the metastable γ phase with dispersed inclusions (Fig. 30). Two specimens (E88 4A, E107 T2A) did show substantial amounts of the cellular transformation product which could not be rationalized on the basis of their thermal history.

For alloys with 6%Mo and higher, the metastable γ phase transformed by the cellular reaction mechanism to α plus enriched γ or $\alpha + \gamma'$ (no distinction will be made here) at aging temperatures of 482°C (900°F) and 566°C (1050°F). Several specimens (E 88 2B,

E101 1A) aged at these temperatures did not show any decomposition of the γ phase but this may well be due to short aging times. In addition, the U-6%Mo-1%Ti alloy aged at 482°C (900°F) exhibited, through etching behavior, the delineation within the matrix of regions transformed by the low temperature mechanism observed in the TTT studies of the 8 and 10%Mo alloys. Hardness measurements of these areas confirmed this.

All of the alloys containing 6 to 10%Mo transformed partially by the high temperature cellular reaction mechanism when furnace cooled from 1700°F (Fig. 30). In general, the amount of the cellular product increased with decreasing Mo content as expected from the observation in the TTT study that the rate of this reaction was lowered by the addition of molybdenum. It was not possible to decide to what extent, if any, the furnace cooled samples had transformed by the low temperature reaction mechanism observed in the TTT study.

Structures of the E106 alloy were difficult to interpret since the TTT diagram for this alloy had not been determined. In addition to the high inclusion content (Fig. 29), the furnace cooled sample exhibited a structure which appeared to contain acicular α (Fig. 32). X-ray data confirmed this and revealed the presence of the γ' phase. Presumably, this alloy would decompose isothermally at high temperatures by the formation of Widmanstatten α in much the same way as was observed in the E105 alloy (see Part I). A lamellar structure was observed in samples quenched from 1300°F to room temperature and aged at 900°F. The isothermal and

aging transformations in this alloy require further study.

Aged specimens of the E105 alloy indicated that quenching and aging influenced the transformation characteristics of this alloy in comparison to isothermally transformed specimens quenched directly to temperature from the γ region. The martensitic transformation which this alloy undergoes on quenching to room temperature is undoubtedly responsible for much of this difference in behavior.

Aging at 566°C (1050°F) produced a fairly extensive cellular mode of decomposition (Fig. 33) as opposed to the primarily Widmanstatten transformation found in the TTT studies (Fig. 28). The degree of decomposition by each of the two modes (cellular and Widmanstatten) is apparently affected by factors such as quenching rate, gammatizing temperature, and aging vs. quenching directly to temperature.

The specimen aged at 370°C (700°F) also showed a peculiar structure (Fig. 34). No such acicular structure was revealed in any of the specimens utilized in the TTT studies. A thorough aging study would be required in order to interpret these structures more completely.

APPENDIX

STANDARD METALLOGRAPHIC PROCEDURES

Mounting - Metallographic specimens were mounted in a commercial cold setting resin.* Resin and specimen were contained within a one-half inch length of one inch diameter Lucite tubing.

Mechanical Polishing - The four steps listed below were utilized for all alloys studied in this investigation.

1.	Belt sander	180 grit	H_2O lubricant
2.	Silicon carbide paper	600 grit	H_2O lubricant
3.	AB Metcloth	8 μ diamond	AB Metadi Fluid
4.	AB Microcloth	Linde B	1% HF solution

Some care must be exercised with the last polishing step since long polishing times may sometimes lead to pitting. If the HF solution is fresh, polishing times will vary from 15 sec to one minute, longer times being required for 6-10%Mo alloys transformed at low temperatures. Mechanical polishing was followed by electrolytic polishing.

Electropolishing - A solution of one part (118g CrO_3: 100ml H_2O) to 4 parts glacial acetic acid, cooled to 2-5°C by means of an ice water bath, was utilized for all alloys. Both cathode and anode were stainless steel and the anode was such as to clamp onto the mounted specimens with a point touching

---

*Hysol Resin #2105 and Hardener #3416.

the polished surface of the metal. An open circuit potential of 50-60 volts D. C. was applied and the specimen polished by repeatedly dipping into the solution 3 to 5 times, each for a duration of about two seconds. Exact voltage was not critical, and in general, longer polishing times were required for alloys of higher molybdenum content.

Two points must be emphasized with respect to standard metallographic techniques. First, before electropolishing is attempted, all surface scratches from polishing operations preceding the Linde B polish must be removed during the final mechanical polish. Second, the specimen must be washed and thoroughly dried before electropolishing.

Etching - In certain instances, the electropolishing procedure described above also produced an etching effect. This was especially true for specimens in which the cellular $\alpha + \gamma$ or the Widmanstatten α transformation products were present. However, in these instances the contrast between the metastable γ phase and the transformation products were usually not satisfactory. In order to increase contrast, the voltage was reduced to 10-12 volts D. C. and the specimen etched for 1-5 seconds. The longer etching times could only be used when the amounts of transformation products were small.

For specimens of 6-10%Mo transformed at low temperatures little was revealed aside from small amounts of the cellular reaction products and the type of oriented figures as shown in Fig. 19. The latter was revealed

by etching for 5-10 seconds at 10-12 volts D. C. and greater contrast produced by further etching for 1-2 seconds at 3 volts. If the alloy had been nearly, or fully transformed at low temperatures, etching at 10-12 volts could only produce a dark staining effect over the entire surface of the specimen.

To reveal the grain structure of specimens either quenched from the gamma phase or transformed at very low temperatures (near 300°C), etching times of 5-15 seconds at 10-12 volts were necessary, the longest time being required for quenched alloys of high molybdenum content.

The Complex E 105 Alloy - Polishing and etching procedures must be modified somewhat for this alloy. For transformation temperatures above the M_s, the Widmanstatten α phase could be observed after electropolishing at 70-80 volts D. C. for 1-4 seconds, the higher voltages and shorter times corresponding to lower temperatures within the range 475-650°C. No further etching was required.

For transformation temperatures below the M_s, polishing was carried out at 60 volts for 2-5 seconds. Any attempts at etching only caused staining of the entire specimen surface.

Anodizing techniques were utilized to reveal the as-quenched structure shown in Fig. 25b. This structure may be faintly seen in the as polished condition under polarized light but was more sharply defined by anodizing. After electropolishing at 60 volts for 3-5 seconds the specimen

was rinsed, dried and then anodized at 20-25 volts D. C. for 1 minute in a solution of 20% ammonium hydroxide and 80% absolute ethyl alcohol. The specimen was held approximately one-half inch away from a nickel cathode. Examination was made under polarized light.

REFERENCES

1. F. A. Rough and A. A. Bauer, "Constitution of Uranium and Thorium Alloys", BMI-1300 (June, 1958).

2. H. A. Saller, F. A. Rough, A. A. Bauer and J. R. Doig, "The Constitution of Delta-Phase Alloys of the System Uranium-Molybdenum-Titanium", BMI-1134 (September, 1956).

3. MS. Farkas, A. A. Bauer, and F. A. Rough, "The Constitution of Delta-Phase Alloys of the System Uranium-Zirconium-Molybdenum", Trans. AIME, 215, (1959) p. 685-693.

4. G. H. Bannister and J. R. Murray, "Some Observation on U-Mo-Nb Alloys", J. Less-Common Metals, 2 (1960) p. 372-382.

5. A. E. Dwight and M. H. Mueller, "Constitution of the Uranium Rich U-Nb and U-Nb-Zr Systems", ANL-5581 (October 1957).

6. R. F. Hills, B. R. Butcher and J. A. Haywood, "A Study of the Effect of Cooling Rate on the Decomposition of the Gamma Phase in Uranium-Low Molybdenum Alloys", J. Less-Common Metals, 3 (April 1961) p. 155-169.

7. K. Tangri, "Les Phases Gamma Metastables dans les Alleages d' Uranium Contenant du Molybdene, Mem. Sci. Rev. Met., 58 (1961) p. 469-477.

8. J. Lehmann and R. F. Hills, "Proposed Nomenclature for Phases in Uranium Alloys", J. Nucl. Materials, 2, (1960) p. 261-268.

9. J. Lehmann, "Study of Phase Transformation Processes in U-Mo Alloys with 0.5 to 4.0 wt%Mo", AEC-tr-4308 (1959).

10. H. A. Saller, F. A. Rough and A. A. Bauer, "Transformation Kinetics of Uranium-Molybdenum Alloys", BMI-957 (October 1954).

11. R. J. VanThyne and D. J. McPherson, "Transformation Kinetics of Uranium-Molybdenum Alloys", Trans. ASM, 49, (1957) p. 598-619.

12. H. Mikhailoff, "Study of Transformations by Annealing of the BCC Gamma Phase of U-Mo Alloys", AEC-tr-4273, (1959).

13. P. C. L. Pfeil and J. D. Browne, "Superlattice Formation in Uranium-Molybdenum Alloys", A. E. R. E. M/R 1333 (1954).

14. E. K. Halteman, "The Crystal Structure of U_2Mo", Acta Cryst., 10, (March 1957) p. 166-169.

15. G. Donze and G. Cabane, "The Decomposition Mechanism of the Gamma Phase in Uranium-Molybdenum and Uranium-Molybdenum-Ruthenium Alloys", SLA Translation 61-16142 (1961).

16. W. A. Hdland, "Isothermal Transformation of U-14 and U-16wt%Mo Alloys at 550°C, NAA-SR-6125 (December 1961).

17. D. Kramer and C. G. Rhodes, "The Gamma to Gamma Prime Transformation in the U-Mo System", NAA-SR-6617 (December 1961).

18. D. Kramer and C. G. Rhodes, "The Precipitation of Metastable Alpha Phase during the Gamma to Gamma Prime Transformation in U-16wt% Mo", Trans. AIME, 224, (October 1962) p. 1015-1020.

19. R. J. VanThyne and D. J. McPherson, "Transformation Kinetics of Uranium-Niobium and Ternary Uranium-Molybdenum-Base Alloys", Trans. ASM, 49, (1957) p. 576-591.

20. A. E. Dwight, "Kinetic Transformations in the Uranium-Rich U-Nb and U-Nb-Zr Systems," ANL-5582 (1957).

21. W. M. Justusson, "Transformation Kinetics of Gamma-Phase Uranium-Molybdenum-Niobium Alloys", J. Nucl. Materials, 4, (1961) p. 37-45.

22. V. W. Storhok, A. A. Bauer and R. F. Dickerson, "Survey of Ternary and Quaternary Metastable Gamma-Phase Uranium Alloys", BMI-1278 (July 1958).

23. A. G. Knapton, "The System Uranium-Titanium", J. Inst. Metals, 83, (1954-55) p. 497.

24. H. A. Saller, R. F. Dickerson and W. E. Murr, "Uranium Alloys for High-Temperature Application", BMI-1098 (June 1956).

25. A. E. Dwight, "The Uranium-Molybdenum Equilibrium Diagram below 900°C", J. Nucl. Materials, 2, (1960) p. 81-87.

26. J. W. Cahn, Acta Metallurgica, 7, (1959) p. 18

27. A. N. Holden, Physical Metallurgy of Uranium, Chap. 14, Addison-Wesley Publishing Company, Inc. (1958)

28. R. F. Dickerson, "Metallography of Uranium", Trans. ASM, 52, (1960), p. 748-762.

29. K. E. G. Meredith and M. B. Waldron, "Inclusions in Uranium Metals", J. Inst. Metals, 87, (1958-59) p. 311-317.

30. A. E. Austin and A. F. Gerds, "The Uranium-Nitrogen Carbon System" BMI-2172 (June 1958)

31. G. L. Kehl, E. Mendel, E. Jaraiz and M. H. Mueller, "Metallographic Identification of Inclusions in Uranium", Trans. ASM, 51, (1959) p. 717-730.

Table I

Critical Temperatures on Heating

(determined by dilatometry)

	$\alpha + \gamma' \rightarrow \alpha + \gamma$	$\alpha + \gamma \rightarrow \gamma$
U-8%Mo	574°C	587°C
U-10%Mo	573°C	580°C

	$\alpha + \gamma' + \varepsilon \rightarrow \alpha + \gamma + \varepsilon$	$\alpha + \gamma + \varepsilon \rightarrow \gamma + \varepsilon$	$\gamma + \varepsilon \rightarrow \gamma$
U-8%Mo-1/2%Ti	577°C	596°C	~ 645°C
U-8%Mo-1%Ti	583°C	635°C	656°C

	$\alpha + \gamma' \rightarrow \alpha + \gamma$	$\alpha + \gamma \rightarrow \gamma$
U-2%Mo-2%Nb-2%Zr-1/2%Ti	600°C	647°C

See Figs. 11, 12, 21 and 24 for phase identification.

Table II

Coefficients of Thermal Expansion
($x10^6$ in/in/°C)

Alloy	Temperature Range 500-575°C	Phase Region
U-10%Mo	18.7	22.0
U-8%Mo	18.8	20.7
U-8%Mo-1/2%Ti	17.5	----
U-8%Mo-1%Ti	20.0	22.9
U-2%Mo-2%Nb-2%Zr-1/2%Ti	23.8	21.7
U-5%Mo*	17.5	19.3
U-7%Mo*	19.3	19.3
U-9%Mo*	16.5	18.7

*Data from Saller et al (24)

Phase Identification in Heat Treated Alloys Received from
U. S. Army Materials Research Agency

TABLE III

Alloy***	Spec. No. and Type	Heat Treatment (°F)	Phases Present*
E88	1A	1300-WQ + 900-AC	ε, γ, ($\alpha+\gamma$)
"	2A	1700-WQ + 900-AC	ε, γ, ($\alpha+\gamma$)
"	3A	As extruded	ε, γ
"	4A	1500-WQ + 400-AC	ε, γ, ($\alpha+\gamma$)
"	5A	1700-WQ	ε, γ
"	1B	1300-WQ + 1050-AC	ε, γ, ($\alpha+\gamma$)
"	2B	1700-WQ + 1050-AC	ε, γ,
"	3B	1700-WQ + 400-AC	ε, γ
"	4B	1500-WQ + 1050-AC	ε, γ, ($\alpha+\gamma$)
"	5B	1700-FC	ε, γ, ($\alpha+\gamma$)
E96	1A	1300-WQ + 900-AC	γ, ($\alpha+\gamma$), ($\alpha+\gamma$)a
"	2A	1500-WQ + 900-AC	γ, ($\alpha+\gamma$), ($\alpha+\gamma$)a
"	3A	1700-WQ + 900-AC	γ, ($\alpha+\gamma$), ($\alpha+\gamma$)a
"	4A	1700-WQ + 400-AC	γ
"	5A	1700-WQ	γ
"	1B	1300-WQ + 1050-AC	γ, ($\alpha+\gamma$)
"	2B	1500-WQ + 1050-AC	γ, ($\alpha+\gamma$)
"	3B	1700-WQ + 1050-AC	γ, ($\alpha+\gamma$)
"	4B	As extruded	γ
"	5B	1700-FC	($\alpha+\gamma$)
E101	1A	1300-WQ + 900-AC	γ
"	2A	1500-WQ + 900-AC	γ, ($\alpha+\gamma$)
"	3A	1700-WQ + 900-AC	γ, ($\alpha+\gamma$)
"	4A	1700-WQ + 400-AC	γ
"	5A	1700-WQ	γ
"	1B	1300-WQ + 1050-AC	γ, ($\alpha+\gamma$)
"	2B	1500-WQ + 1050-AC	γ, ($\alpha+\gamma$)
"	3B	1700-WQ + 1050-AC	γ, ($\alpha+\gamma$)
"	4B	As extruded	γ
"	5B	1700-FC	γ, ($\alpha+\gamma$)

---

* The following designation has been used:

($\alpha+\gamma$): cellular, or lamellar ($\alpha+\gamma$)

($\alpha+\gamma$)a: oriented, or low temperature ($\alpha+\gamma$) not revealed metallographically

α_m : martensitic α

α_a : acicular, or Widmanstatten α characteristic of E105 alloy

Alloy***	Spec. No. and Type	Heat Treatment (°F)	Phases Present*
E103	1A	1300-WQ + 400-AC	γ
"	2A	1300-WQ + 1050-AC	γ, $(\alpha+\gamma)$
"	5A	1700-WQ	γ
"	1B	As extruded	γ
"	2B	1300-WQ + 900-AC	γ, $(\alpha+\gamma)$
"	5B	1700-FC	γ, $(\alpha+\gamma)$
E105	1A	As extruded	γ, α_m
"	5A	1700-FC	γ, α_a, BCC
"	1B	1700-WQ	γ, α_m
"	2B	1700-WQ + 1050-AC	γ, α_a, $(\gamma+\alpha)$
"	3B	1500-WQ + 1050-AC	γ, α_a, $(\alpha+\gamma)$
"	4B	1300-WQ + 1050-AC	γ, α_a, $(\alpha+\gamma)$
"	5B	1500-WQ + 700-AC	γ, α_a, BCC
E106	1A	As extruded	γ , VN****
"	2A	1700-FC	VN, γ'
"	3A	1700-WQ	γ **, VN
"	5A	1500-WQ + 600-AC	γ , VN, $(\alpha+\gamma)_a$
"	3B	1700- oil	γ , VN
"	4B	1500-WQ + 700-AC	γ , VN, $(\alpha+\gamma)_a$
"	5B	1300-WQ + 900-AC	γ , VN $(\alpha+\gamma)$
E107	T1	As extruded	γ
"	T2	As extruded	γ
"	T2A	1700-WQ	γ, $(\alpha+\gamma)$
"	B1	As extruded	γ
"	B2	As extruded	γ
"	B2B	1700-FC	-
E108	---	As extruded	γ
E111	---	"	γ
E119	---	"	γ
E120	---	"	γ
E139	---	"	γ
RL52	---	"	γ, α_m
RL55	---	"	γ, VN

** Absence of γ transformation checked by x-ray diffraction.
*** See page 25 for compositions.
****Vanadium Nitride

Distribution List

No. of Copies	To
	Commanding Officer Watertown Arsenal Watertown 72, Massachusetts
5	Attn: ORDBE-LX
1	ORDBE-EL
1	Commanding Officer Ordnance Materials Research Office Watertown Arsenal Watertown 72, Massachusetts Attn: RPD
1	Office, Chief of Ordnance Department of the Army Washington 25, D. C. Attn: ORDTB-Res. & Materials
1	Director Army Research Office Department of the Army Washington 25, D. C.
	Commanding General Ordnance Weapons Command Rock Island, Illinois
1	Attn: ORDOW-IX
2	Attn: ORDOW-TX
	Commanding General Aberdeen Proving Ground Aberdeen, Maryland
1	Attn: Ballistic Research Lab.
1	Attn: ORDBG-LH, Tech Library, Bldg. 313
	Commanding General Army Ballistic Missile Agency Redstone Arsenal, Alabama
1	Attn: ORDAB-DRF, Mr. W. A. Wilson
5	Attn: ORDAB-DSN, Dr. W. R. Lucas

	Commanding General Army Rocket & Guided Missile Agency Redstone Arsenal, Alabama
1	Attn: ORDAB-DV
5	Attn: ORDXR-OCP, Mr. R. L. Wetherington
	Commanding Officer Detroit Arsenal Center Line, Michigan
1	Attn: ORDMX-BMW ORDMX-AL
	Commanding Officer Diamond Ordnance Fuze Laboratories Washington 25, D. C.
1	Attn: ORDTL 06.33, Technical Reference Section
	Commanding Officer Frankford Arsenal Bridge-Tacony Streets Philadelphia 37, Pennsylvania
2	Attn: Pitman-Dunn Labs.
	Commanding Officer Ordnance Ammunition Command Joliot, Illinois
1	Attn: ORDLY-AR
	Commanding General Ordnance Tank-Automotive Command 1501 Beard Street Detroit 9, Michigan
1	Attn: ORDMC-RM. 1
	Commanding General Ordnance Tank-Automotive Command Detroit Arsenal Center Line, Michigan
1	Attn: ORDMC-RM. 1, Mr. Charles Salter
	Commanding Officer Picatinny Arsenal Dover, New Jersey
1	Attn: FREL

	Commanding Officer Redstone Arsenal Redstone Arsenal, Alabama
1	Attn: Technical Library
	Commanding Officer Rock Island Arsenal Rock Island, Illinois
1	Attn: Laboratory
	Commanding Officer Springfield Armory Springfield 1, Massachusetts
1	Attn: ORDBD-TX
	Commanding General U. S. Army Ordnance Special Weapons Ammunition Command
1	Dover, New Jersey
	Commanding Officer Watervliet Arsenal Watervliet, New York
1	Attn: ORDBF-RT
	Cognizant Ordnance District
1	(for contracts only)
	The Director Jet Propulsion Laboratory California Institute of Technology Pasadena 3, California
1	Attn: Dr. L. Jaffe
	Commanding Officer Office of Ordnance Research Box CM, Duke Station Durham, North Carolina
1	Attn: ORDOR-ED
1	Attn: Dr. Peter Konting
	Army Reactor Branch Division of Research Development Atomic Energy Commission
1	Washington 25, D. C.

	Director Army Research Office Department of the Army
1	Washington 25, D. C.
	Commander Armed Services Tech. Info. Agency Arlington Hall Station Arlington 12, Virginia
10	Attn: TIPDR
	Chief Bureau of Aeronautics Department of the Navy Washing ton 25, D. C.
1	Attn: TD Division
	Chief, Bureau of Ordnance Department of the Navy Washington 25, D. C.
1	Attn: Rep-3
	Chief, Bureau of Ships Department of the Navy Washington 25, D. C.
1	Attn: Code 592
	Chief, Naval Eng. Exp. Station Department of the Navy
1	Annapolis, Maryland
	Commander Naval Proving Ground Dahlgren, Virginia
1	Attn: A & P Lab.
	Director Naval Research Laboratory Anacostia Station Washington 25, D. C.
1	Attn: Technical Information Officer
	Chief, Office of Naval Research Department of the Navy Washington 25, D. C.
1	Attn: Code 423

	Commander Wright Air Development Center Wright-Patterson Air Force Base, Ohio
1	Attn: WCTRO
1	Attn: WCRRL
	U. S. Atomic Energy Commission Technical Information Service Extension P. O. Box 62
15	Oak Ridge, Tennessee
	National Aeronautics and Space Administration 1520 H Street, N. W.
1	Washington 25, D. C.
	Research Division Library Raytheon Company 28 Seyon Street
1	Waltham 54, Massachusetts
	Defense Metals Information Center Battelle Memorial Institute Columbus, Ohio (Uncl Rots Only) Classified reports to be forwarded: Commanding Officer Ordnance Materials Research Office Watertown Arsenal 72, Mass.
1	Attn: PS&C Div for Transmittla to DMIC

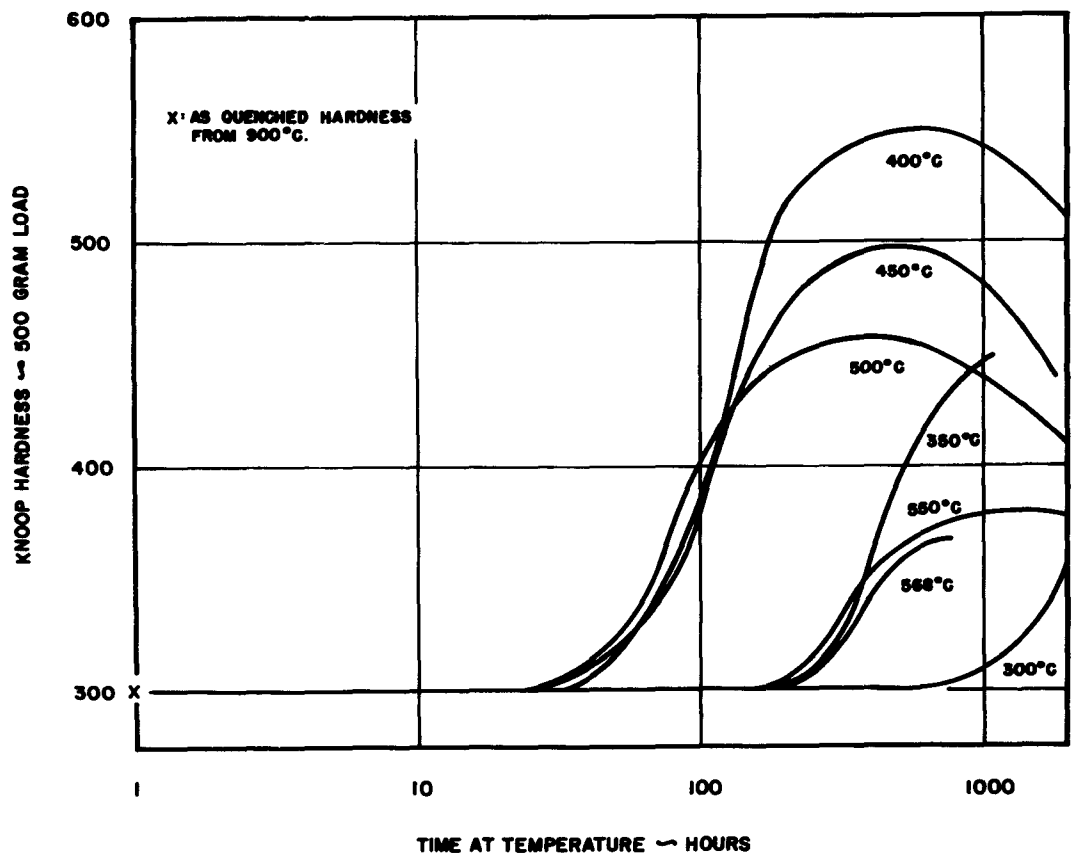

FIG.1: ISOTHERMAL HARDNESS CURVES FOR ALLOY E 139 QUENCHED TO TEMPERATURE FROM 900°C. (1650°F) —— E 139 —— 10% Mo

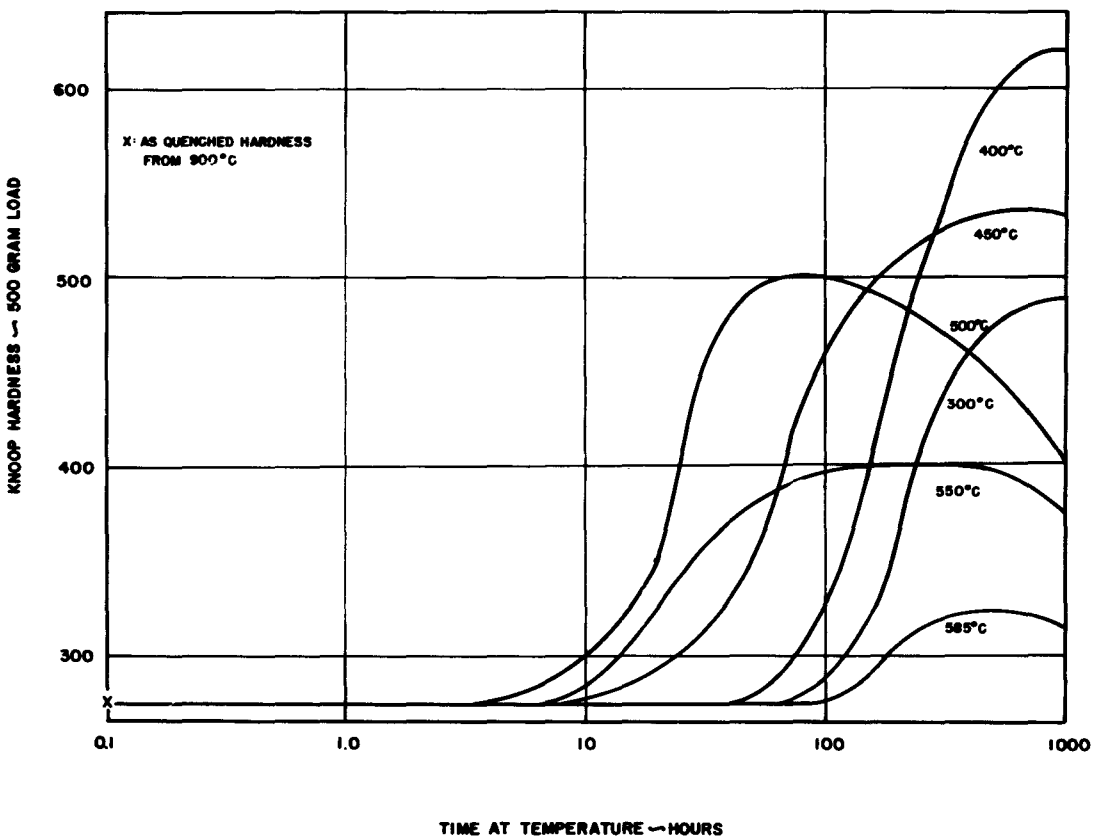

FIG.2 : ISOTHERMAL HARDNESS CURVES FOR ALLOY E101 QUENCHED TO TEMPERATURE FROM 900°C (1650°). —— E101 – 8% Mo

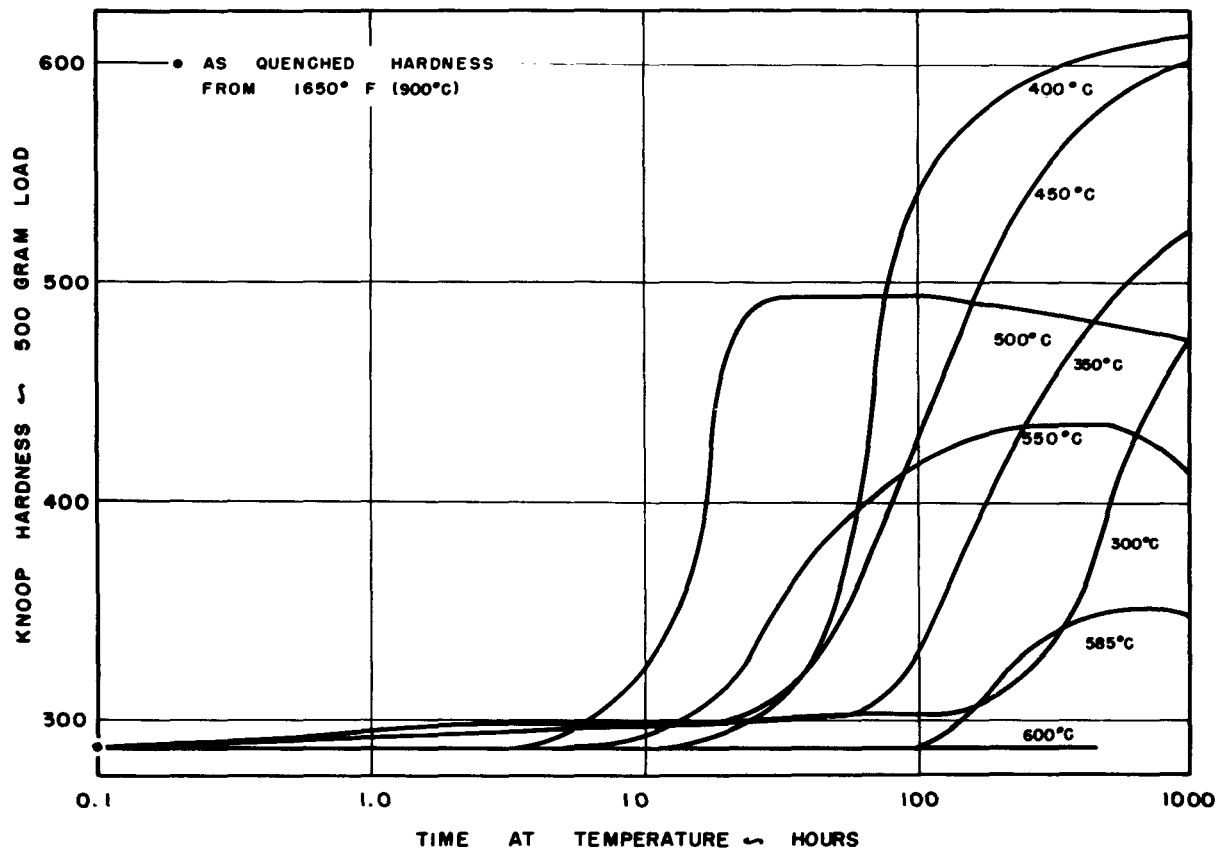

FIG. 3: ISOTHERMAL HARDNESS CURVES FOR ALLOY E 107 QUENCHED TO TEMPERATURE FROM 900°C (1650°F).- E 107 — 8% — $\frac{1}{2}$ % Ti

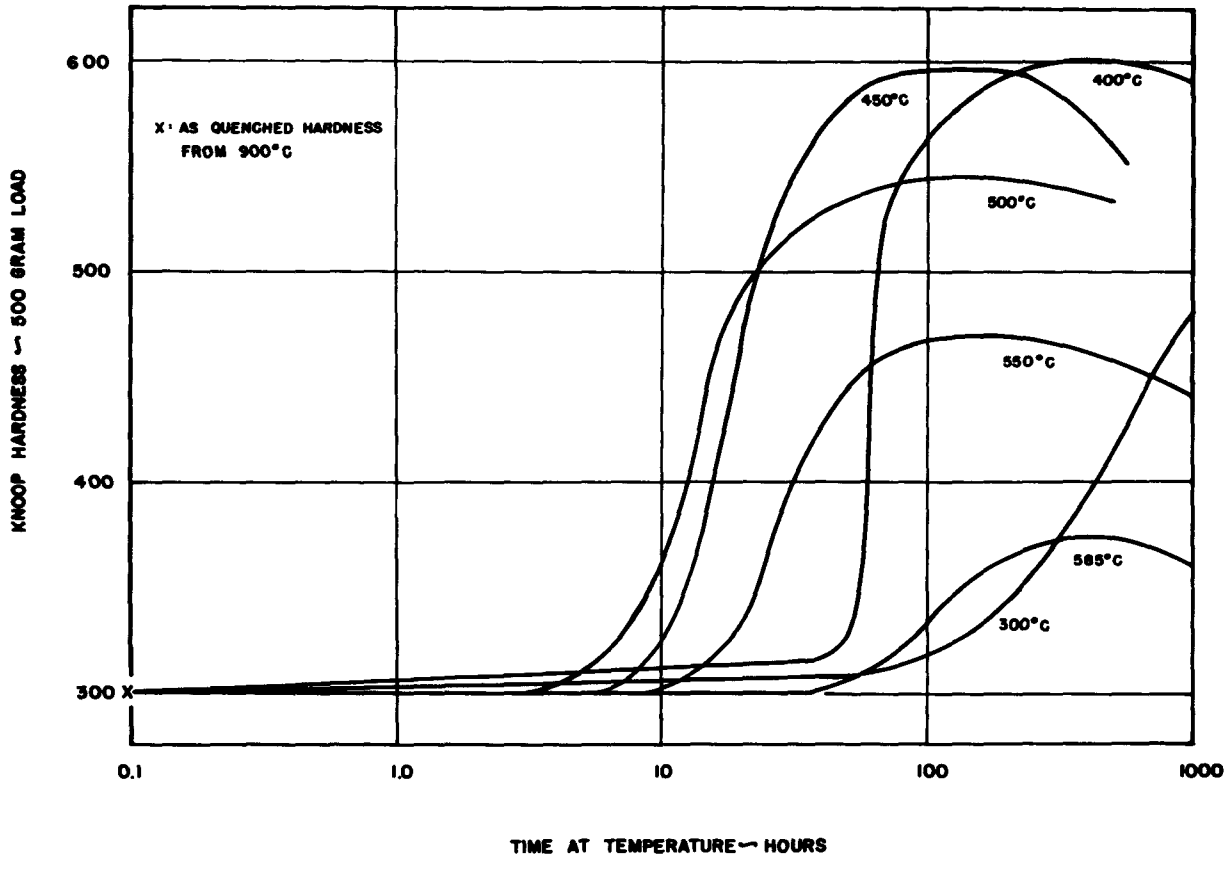

FIG. 4 : ISOTHERMAL HARDNESS CURVES FOR ALLOY E88 QUENCHED TO TEMPERATURE FROM 900°C (1650°). —— E88 — 8% Mo — 1% Ti

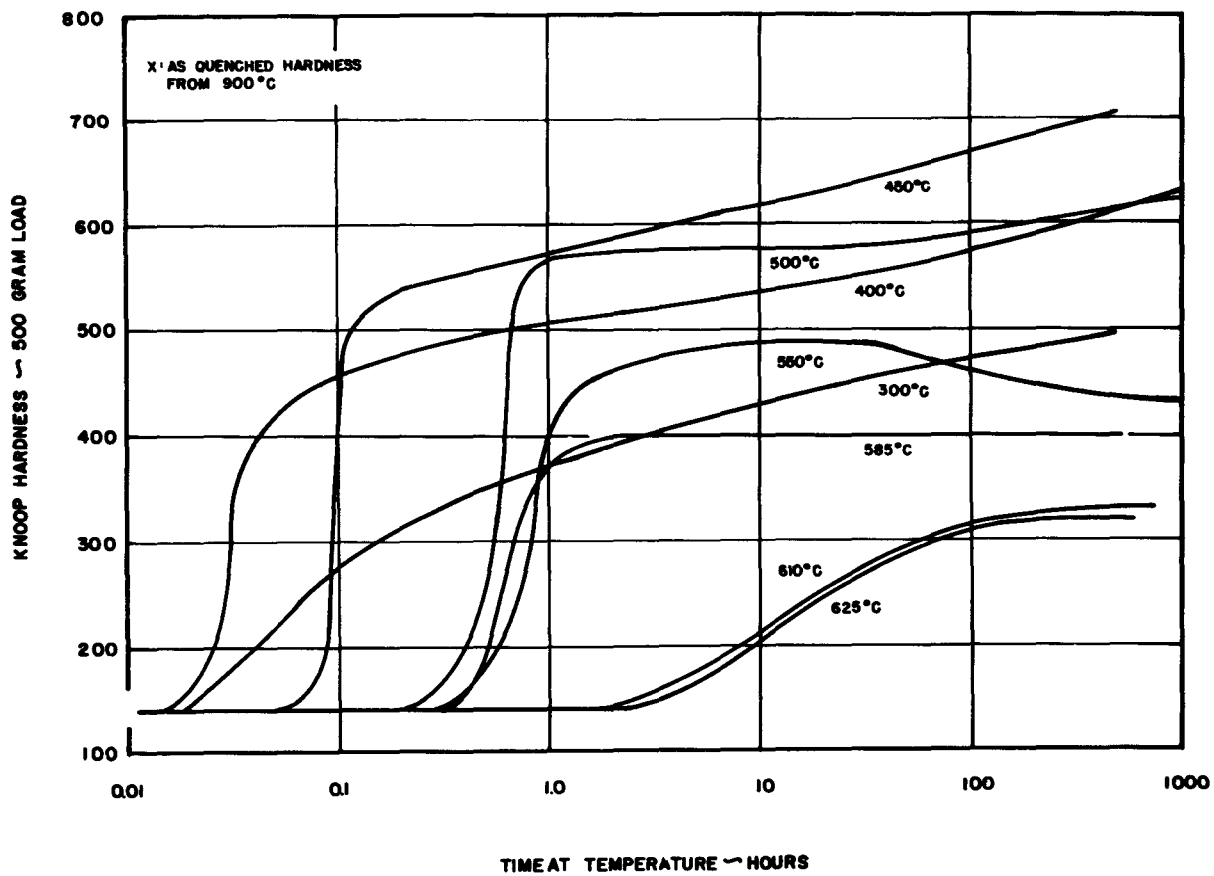

FIG. 5: ISOTHERMAL HARDNESS CURVES FOR ALLOY E 105 QUENCHED TO TEMPERATURE FROM 900°C (1650°F). — E 105 — 2% Mo — % Ti — 2% Nb — 2% Zr

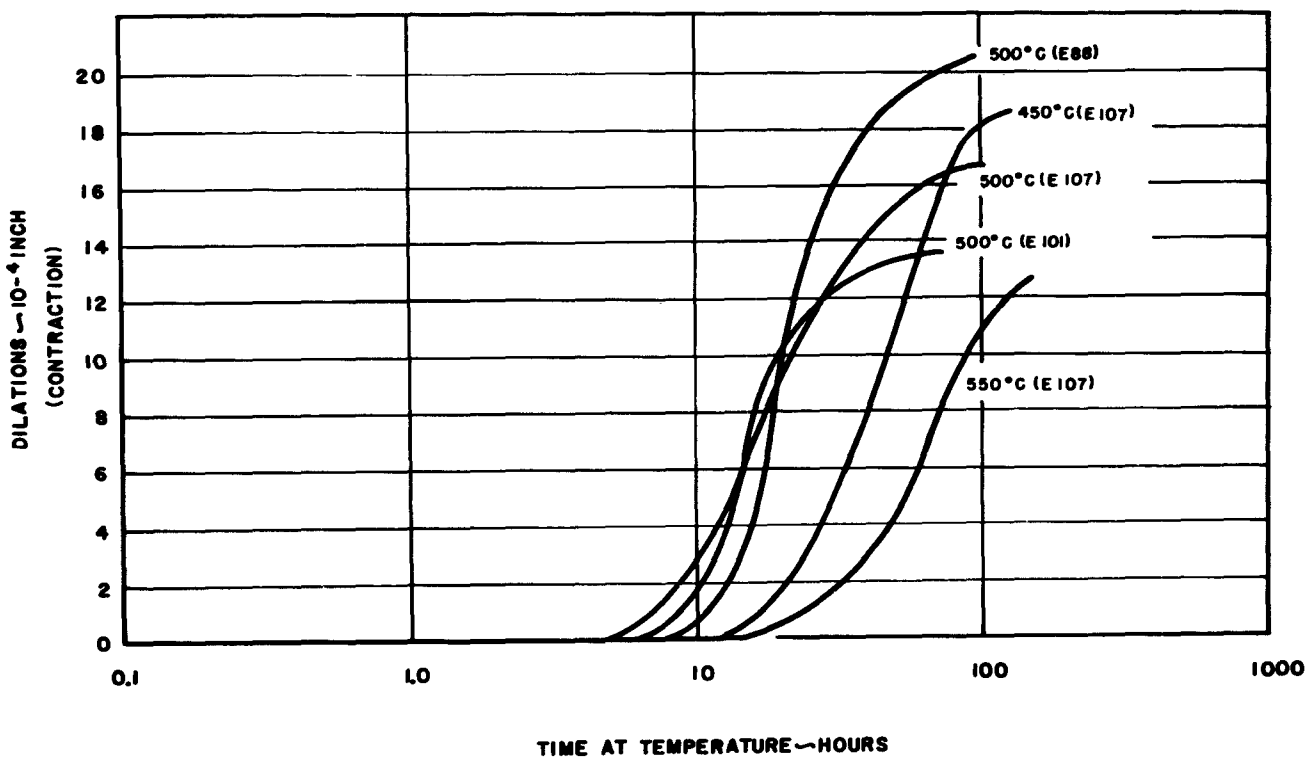

FIG. 6: EFFECT OF HOLDING TIME ON THE DILATION OF ALLOYS E88, E101 AND E107 QUENCHED TO TEMPERATURE FROM 900°C.

E88 — 8% Mo – 1% Ti
E101 — 8% Mo
E107 — 8% Mo – $\frac{1}{2}$% Ti

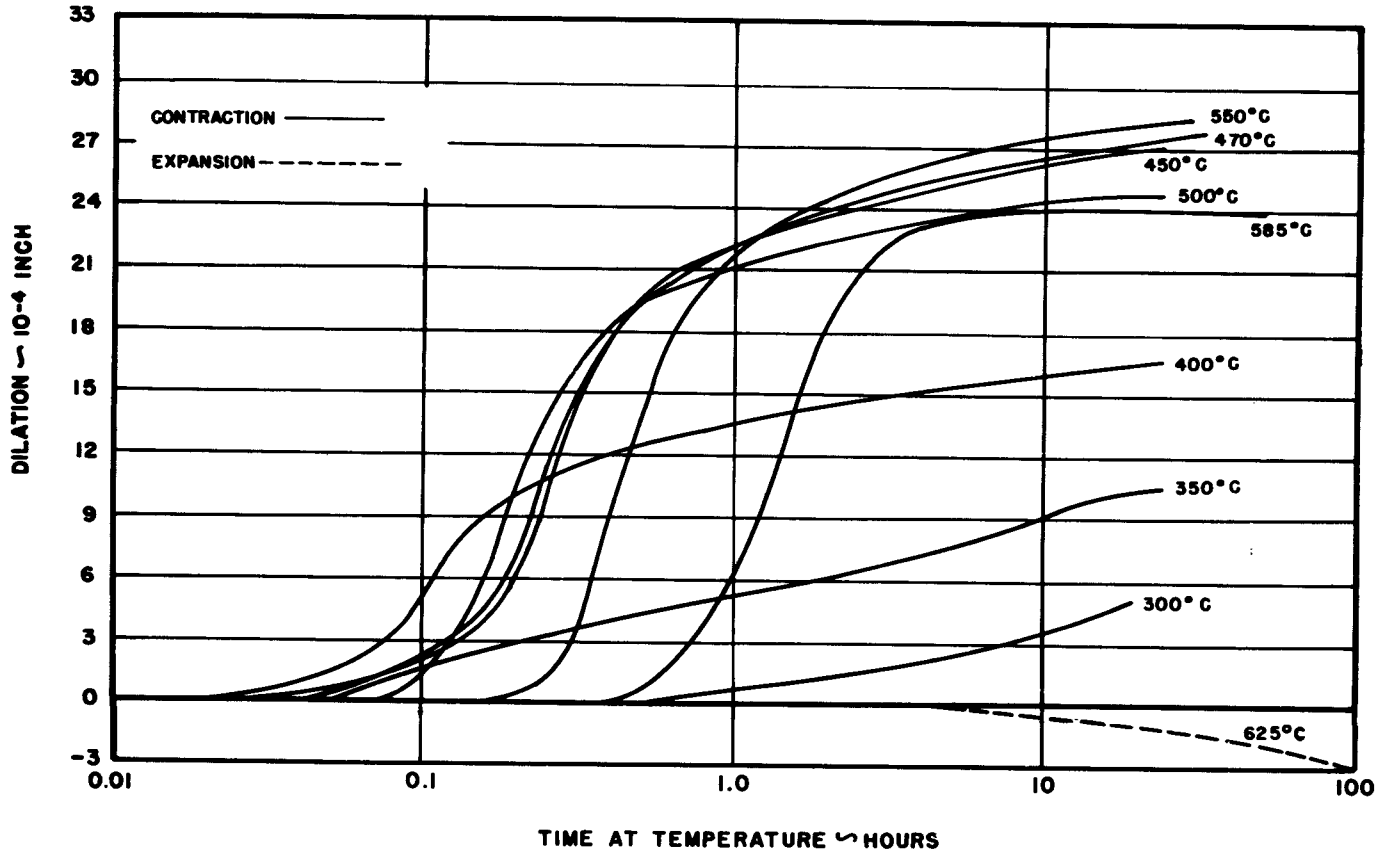

FIG. 7: EFFECT OF HOLDING TIME ON THE DILATION OF ALLOY E105 QUENCHED TO TEMPERATURE FROM 900°C —— E105 — 2% Mo — $\frac{1}{2}$% Ti — 2% Nb — 2% Zr

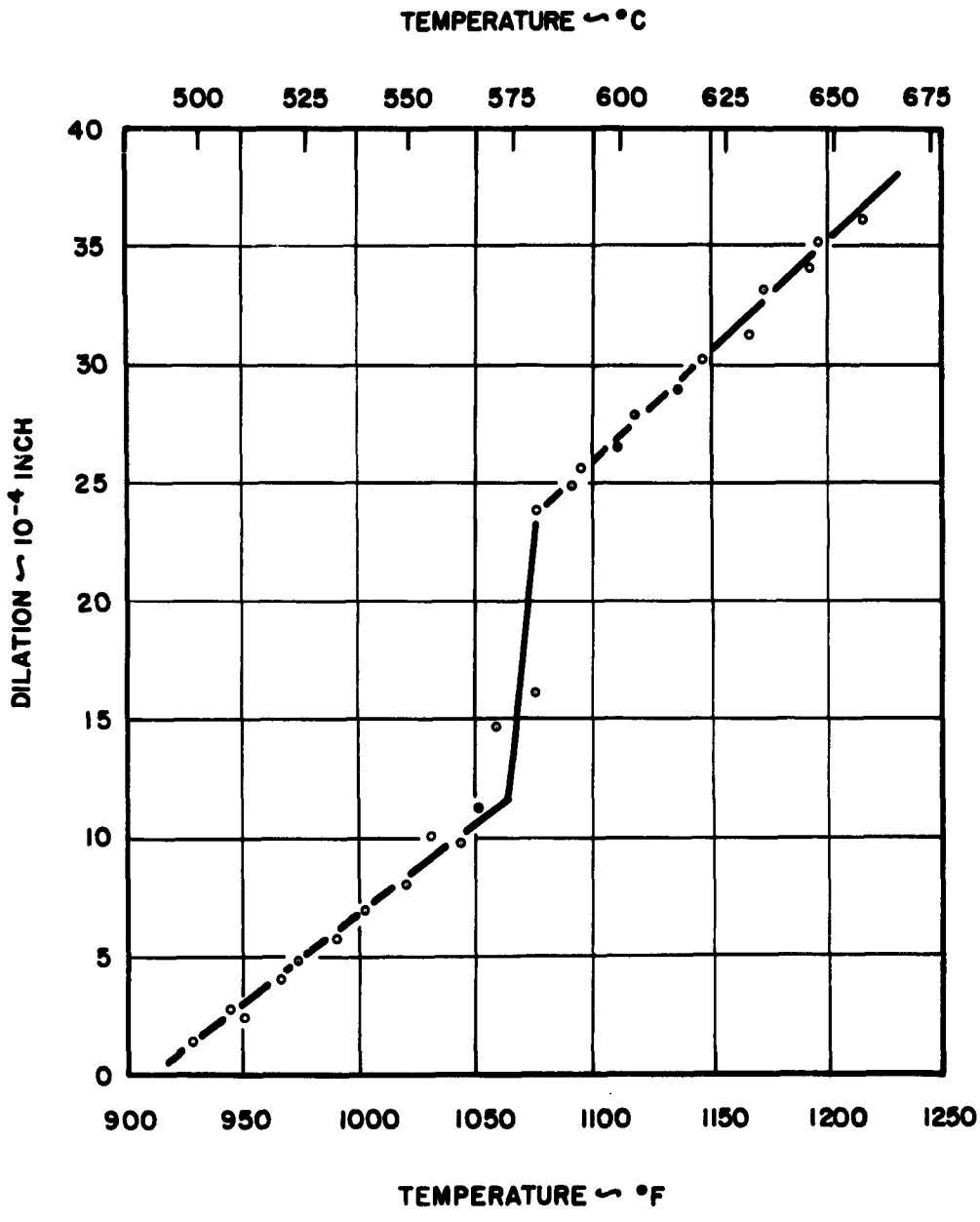

FIG.8: EFFECT OF TEMPERATURE ON THE DILATION OF ALLOY E 139. —— 10% Mo

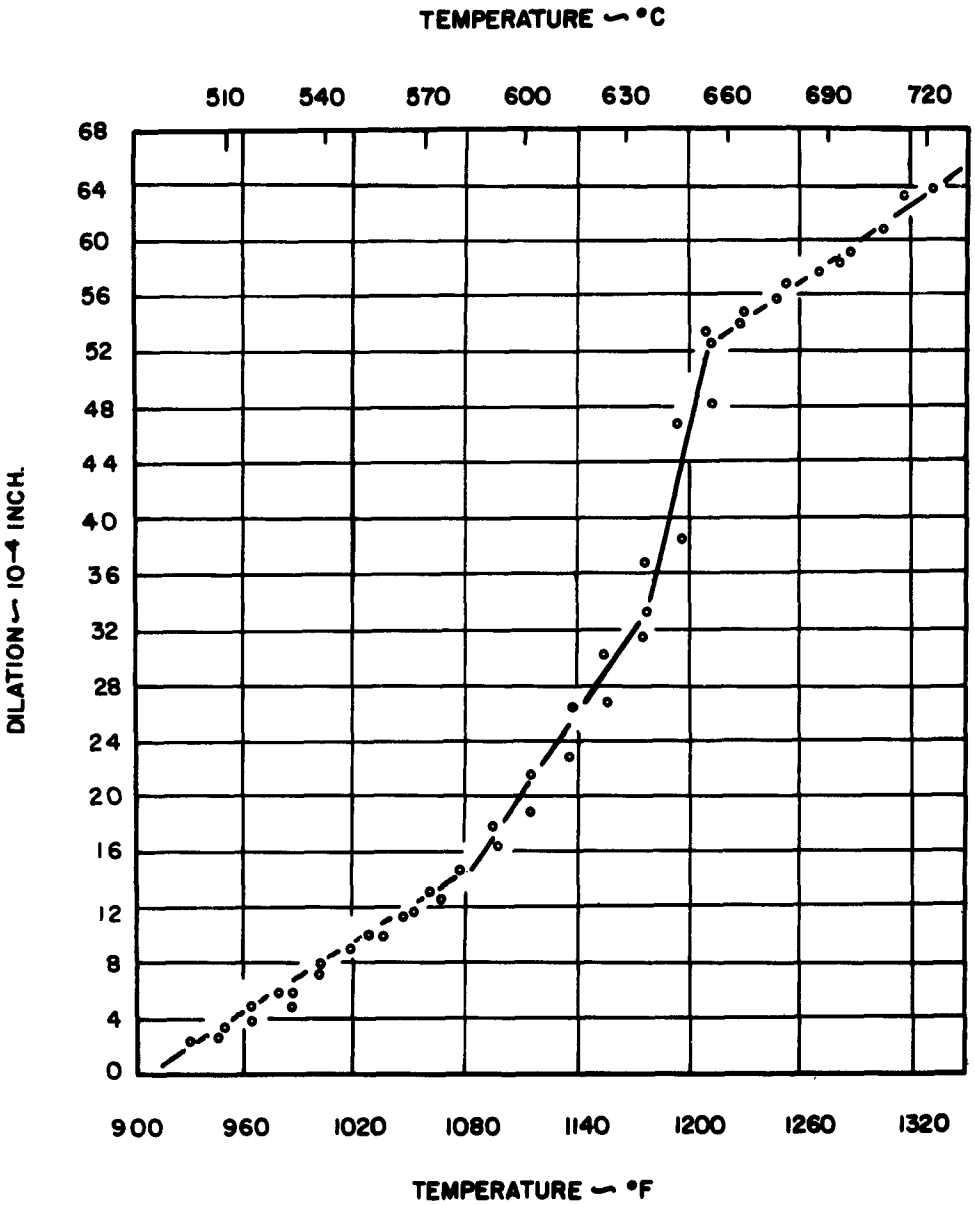

FIG. 9 : EFFECT OF TEMPERATURE ON THE DILATION OF ALLOY E88. —— 8% Mo – 1% Ti

FIG. 10: U-10% Mo. WATER QUENCHED FROM 900°C. X100

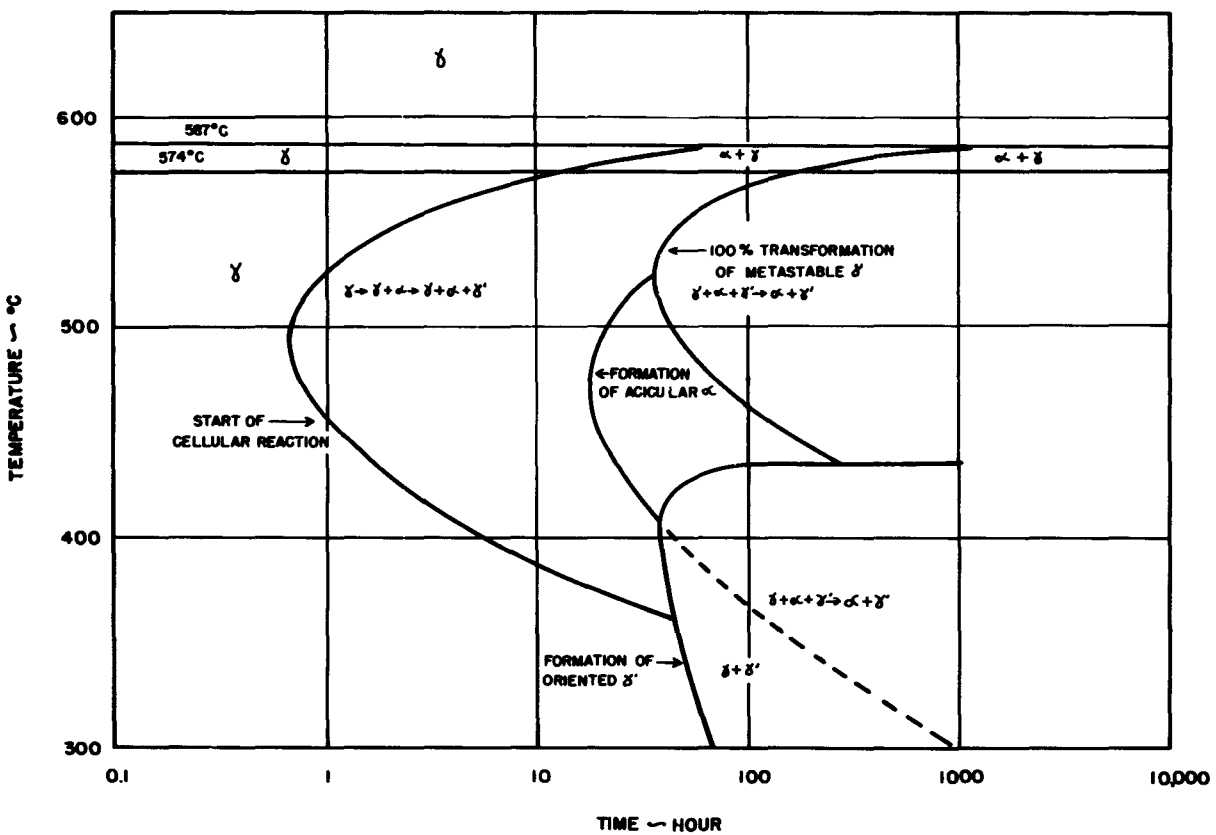

FIG.11: TTT DIAGRAM FOR THE U- 8% Mo ALLOY QUENCHED TO TEMPERATURE FROM 900°C (1650°F).

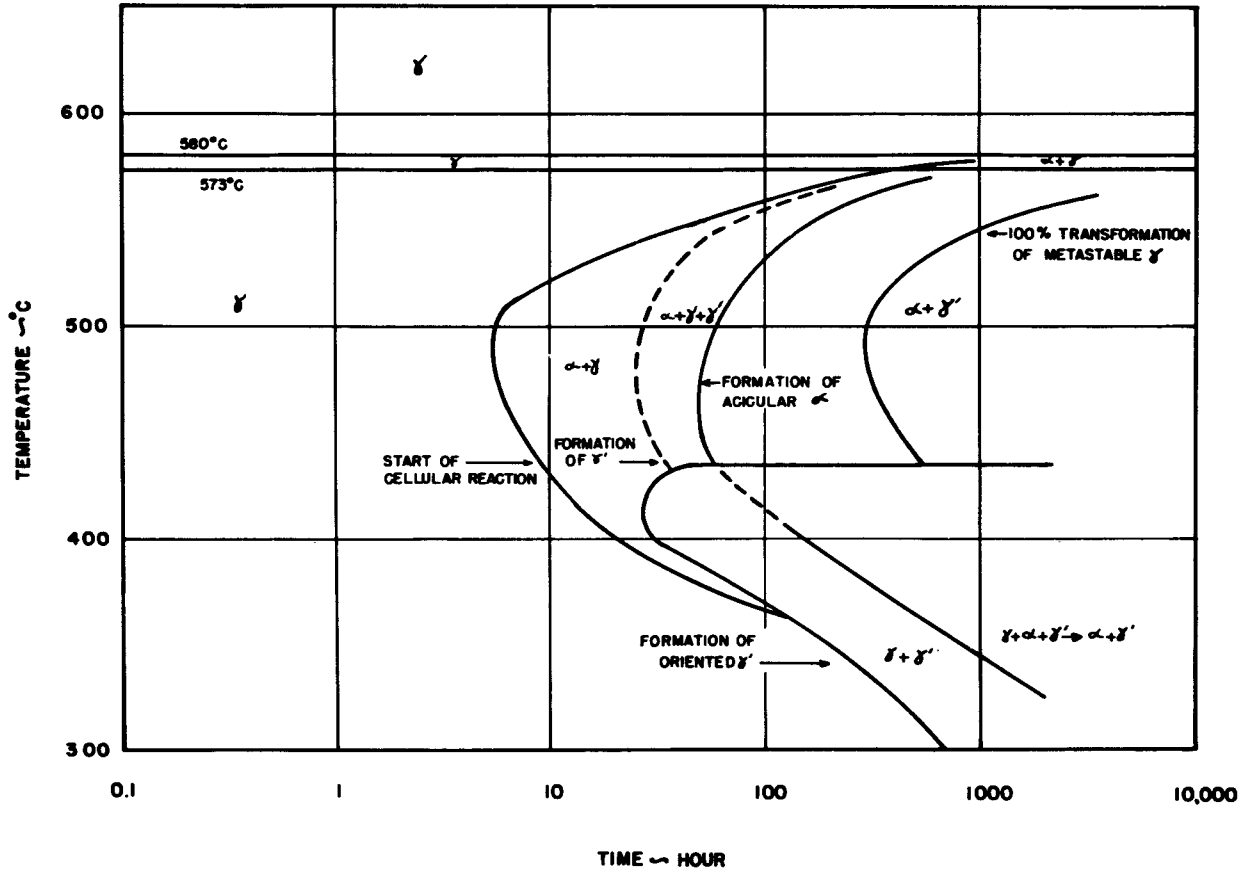

FIG. 12 - TTT DIAGRAM FOR THE U-10% Mo ALLOY QUENCHED TO TEMPERATURE FROM 900°C (1650 °F).

a. 24 HR AT 550°C,
WATER QUENCHED
X 250

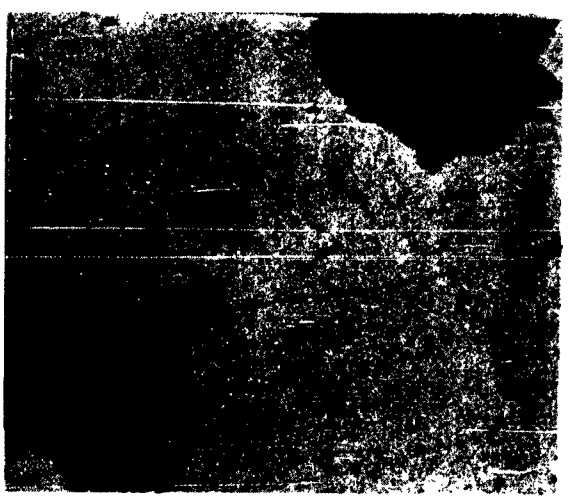

b. 240 HR AT 550°C,
WATER QUENCHED
X 250

FIG. 13 : U-10% Mo QUENCHED FROM 900°C TO 550°C AND HELD ISOTHERMALLY.
ILLUSTRATION OF CELLULAR REACTION ON TRANSFORMATION

(SEE FIG. 12)

FIG. 14 : U-8% Mo. QUENCHED FROM 900°C TO 585°C, HELD ISOTHERMALLY FOR 1000 HR, WATER QUENCHED. X500
ILLUSTRATION OF TRANSFORMATION IN ADVANCED STAGE.

(SEE PAGE II)

a. 22 HR AT 450°C,
WATER QUENCHED
X 100

b. 50 HR AT 450°C,
WATER QUENCHED
X100

c. 98 HR AT 450°C,
WATER QUENCHED
X100

FIG. 15 : U- 8 % Mo. QUENCHED FROM 900 °C TO 450°C
AND HELD ISOTHERMALLY.
CELLULAR MODE OF TRANSFORMATION AT
VARIOUS STAGES OF COMPLETION

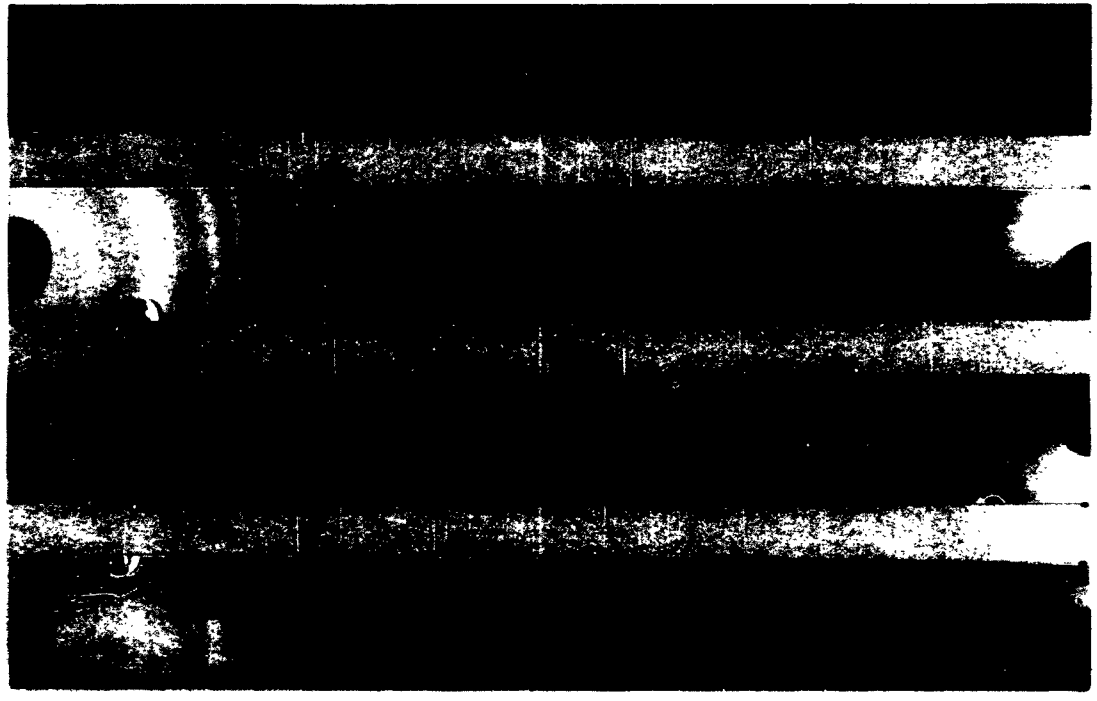

a. WATER QUENCHED FROM 900°C ($K_\alpha + K_\beta$)

b. 1000 HR AT 500°C, WATER QUENCHED

c. 98 HR AT 400°C, WATER QUENCHED

d. 1000 HR AT 400°C, WATER QUENCHED

FIG. 16 : U – 10 % Mo. DEBYE X-RAY PATTERNS. Cu – K_α RADIATION. SPECIMENS QUENCHED TO TEMPERATURE FROM 900°C AND ISOTHERMALLY TRANSFORMED.
X-RAY EVIDENCE OF TRANSFORMATION MORPHOLOGY

(SEE PAGE 16)

FIG. 17 : U-10% Mo. QUENCHED FROM 900°C TO 450°C, HELD ISOTHERMALLY FOR 1000 HR, WATER QUENCHED. X 100

FIG. 18 : U- 10% Mo. QUENCHED FROM 900° C TO 400° C, HELD ISOTHERMALLY FOR 1000 HR, WATER QUENCHED. X 100

ILLUSTRATIONS OF LOW TEMPERATURE TRANSFORMATION

(SEE PAGE 17)

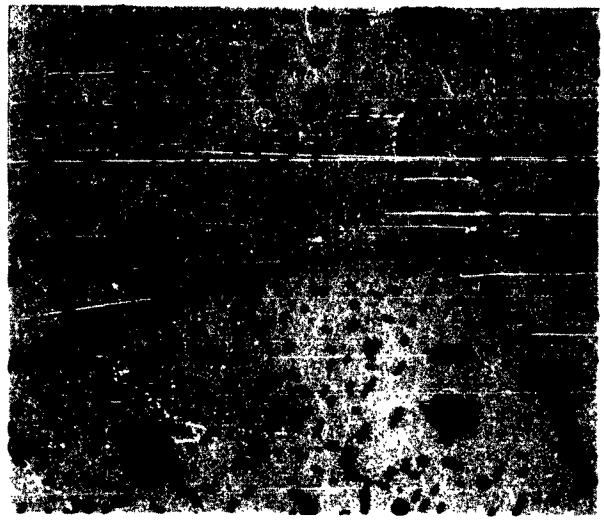

FIG. 19: U-10 % Mo. QUENCHED FROM 900°C TO 400°C, HELD ISOTHERMALLY FOR 98HR, WATER QUENCHED. X1000
ILLUSTRATION OF LOW TEMPERATURE TRANSFORMATION.

(SEE PAGE 17)

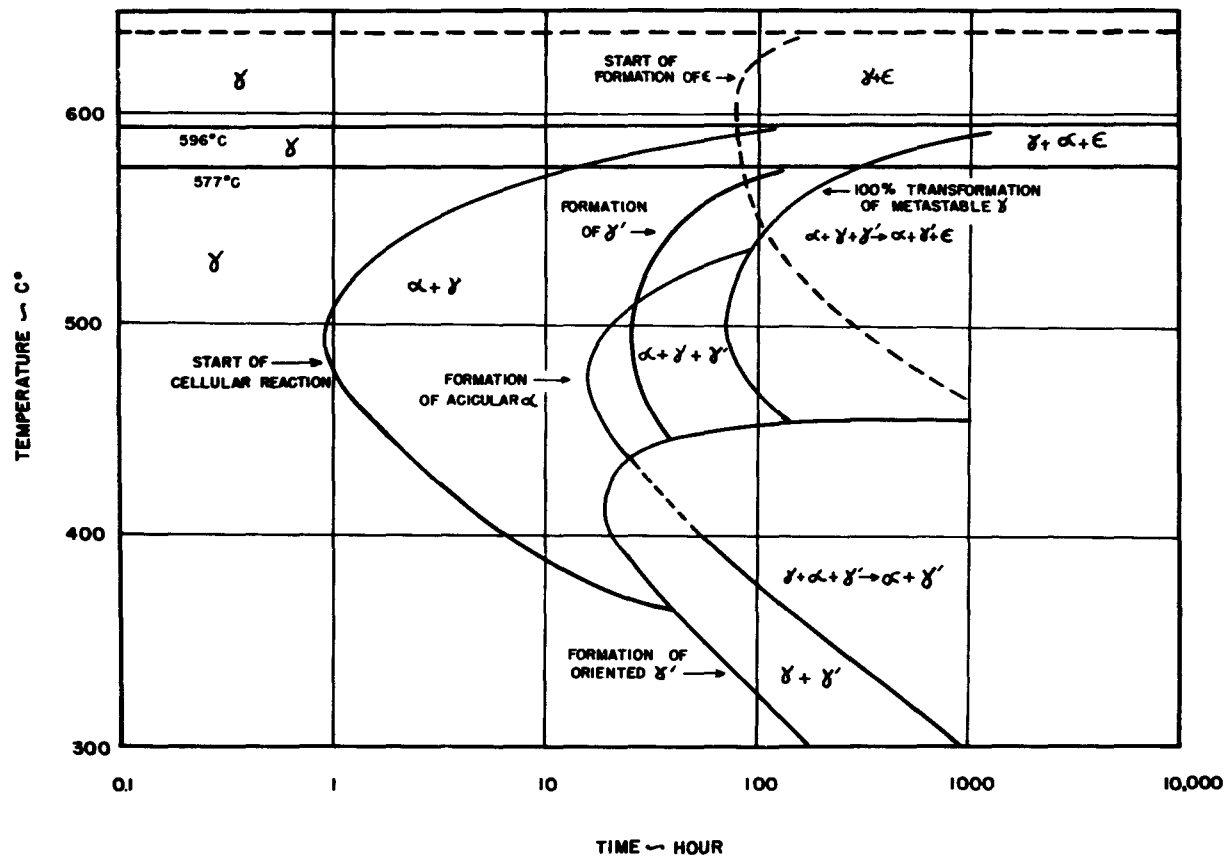

FIG. 20: TTT DIAGRAM FOR THE U-8% Mo-$\frac{1}{2}$% Ti ALLOY QUENCHED TO TEMPERATURE FROM 900°C (1650°F).

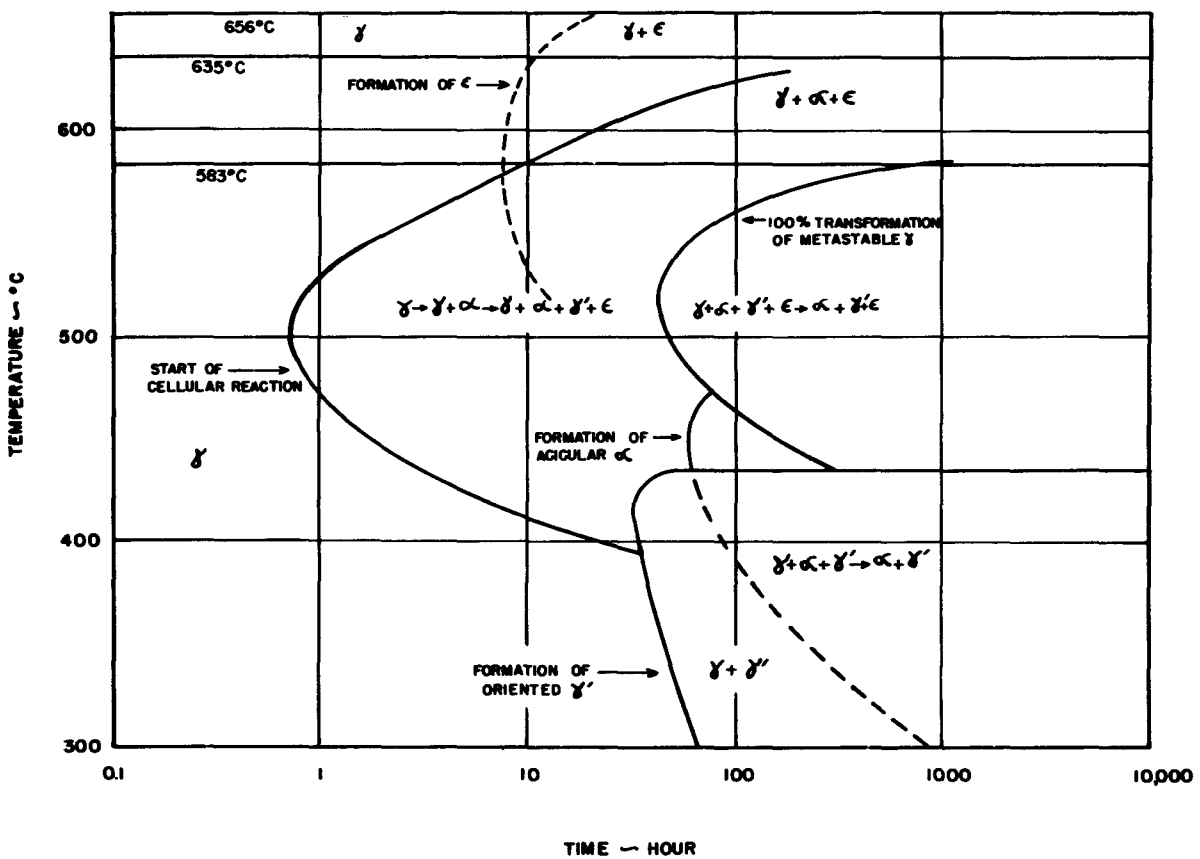

FIG. 21: TTT DIAGRAM FOR THE U-8% Mo-1% Ti ALLOY QUENCHED TO TEMPERATURE FROM 900°C (1650° F).

a. U- 8% Mo- $\frac{1}{2}$ %Ti

X100

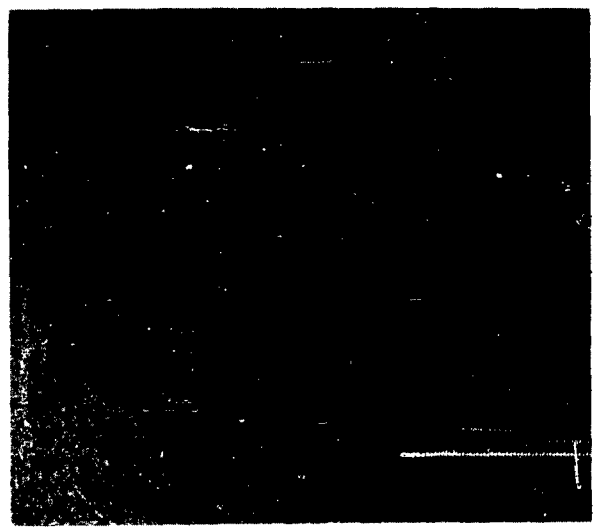

b. U- 8% Mo- 1% Ti

X100

FIG. 22 : U-8% Mo- $\frac{1}{2}$ % Ti AND U-8 % Mo- 1% Ti
WATER QUENCHED FROM 900°C.
ILLUSTRATION OF Ti RICH PRECIPITATES

(SEE PAGE 19)

FIG. 23 : U - 8 % Mo - $\frac{1}{2}$ % Ti. QUENCHED FROM 900°C TO 600°C, HELD ISOTHERMALLY FOR 500 HR, WATER QUENCHED. X200 ILLUSTRATION OF Ti RICH PRECIPITATES AT ADVANCED STAGE OF TRANSFORMATION

(SEE PAGE 19)

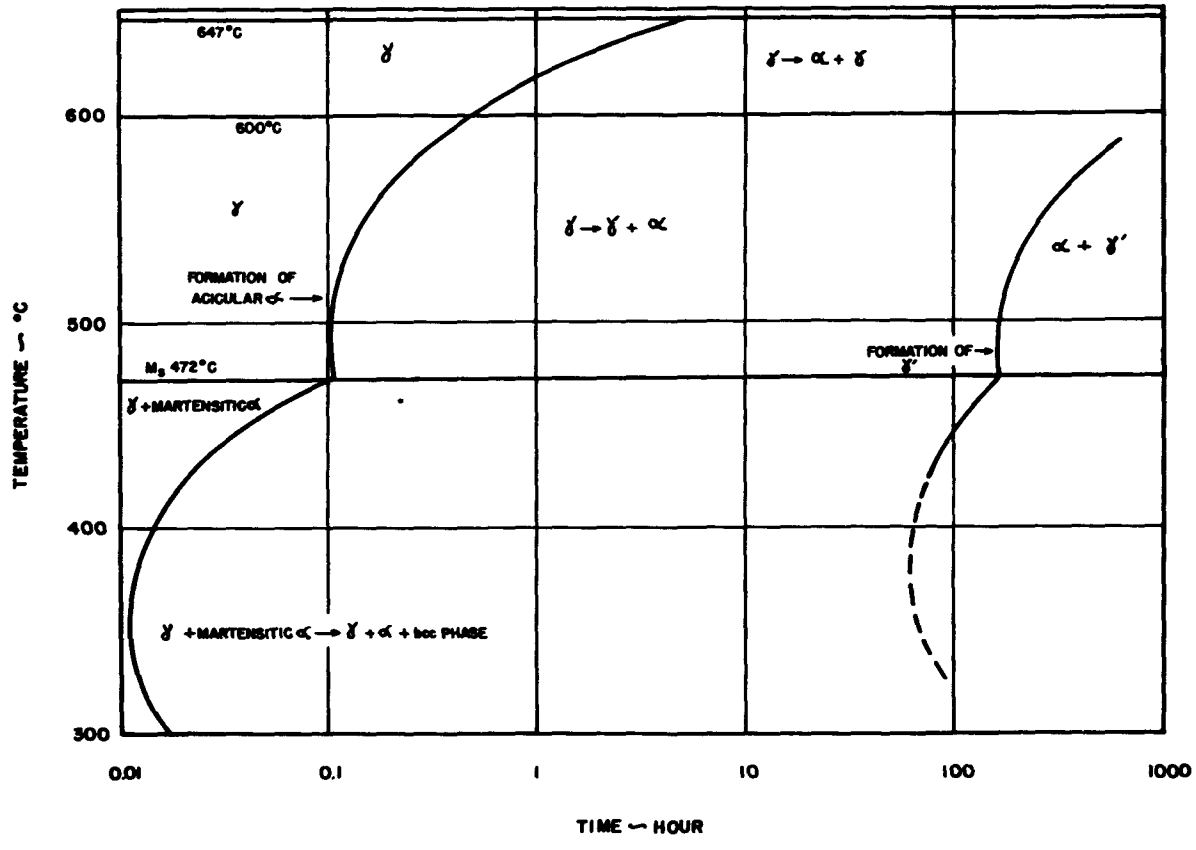

FIG.24: TTT DIAGRAM FOR THE U-2% Mo-2% Nb-2% Zr-$\frac{1}{2}$%Ti ALLOY QUENCHED TO TEMPERATURE FROM 900°C (1650°F).

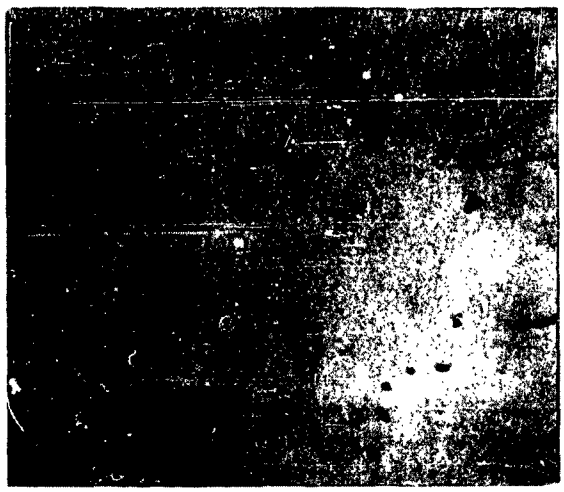

a. ANODIZED, VIEWED IN BRIGHT LIGHT. X500

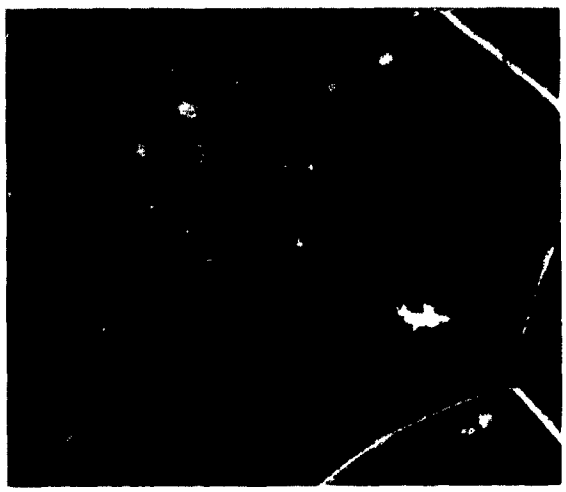

b. ANODIZED, VIEWED IN POLARIZED LIGHT. X500

FIG. 25 : U-2 % Mo - 2% Nb - 2% Zr - $\frac{1}{2}$ % Ti. WATER QUENCHED FROM 900°C. POSSIBLE MARTENSITIC PHASE

(SEE PAGE 21)

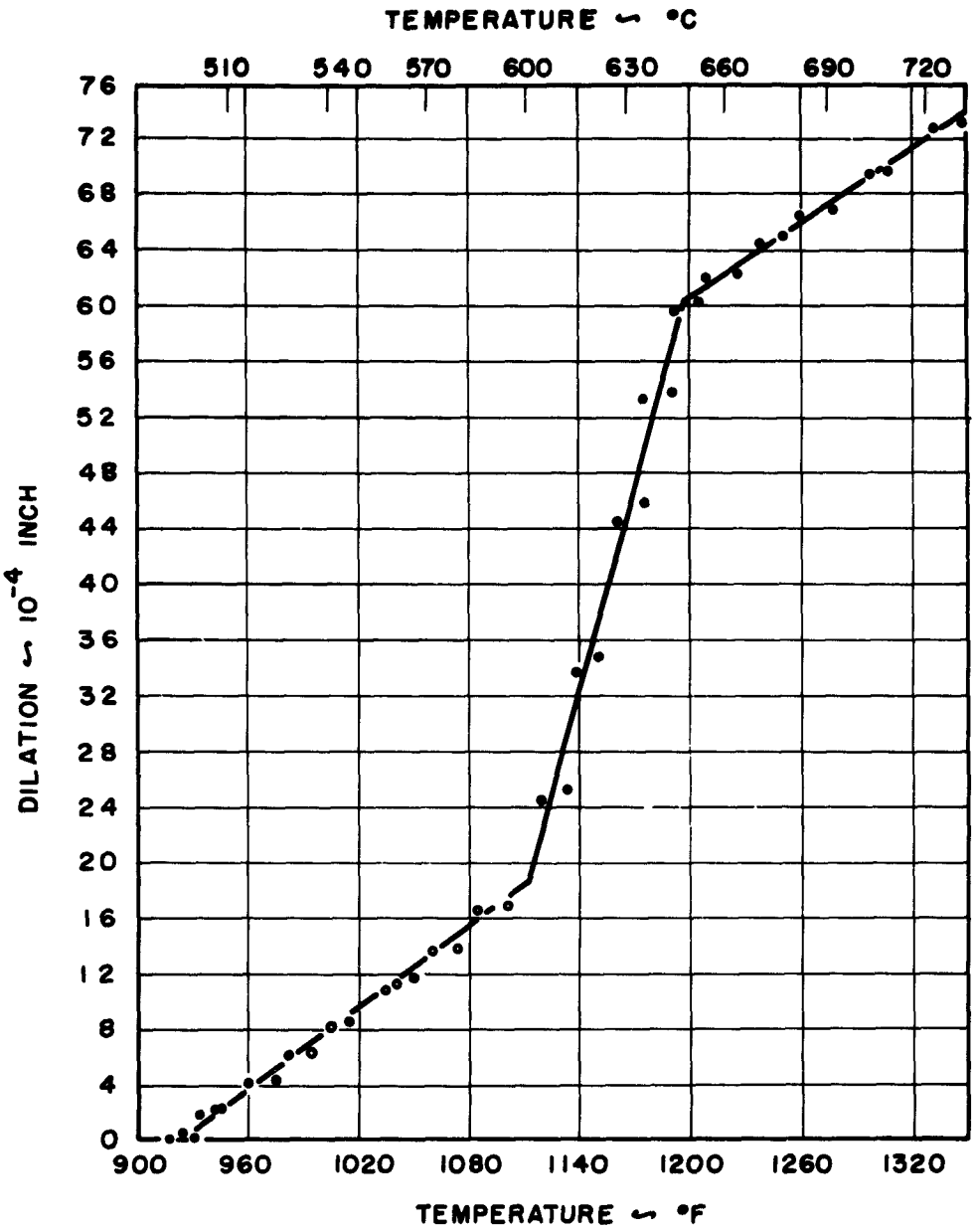

FIG. 26 : EFFECT OF TEMPERATURE ON THE DILATION OF ALLOY E 105 .— 2% Mo – $\frac{1}{2}$% Ti – 2% Nb – 2% Zr

ADVANCED STAGE
OF TRANSFORMATION

FIG. 27: U - 2% Mo - 2% Nb - 2% Zr - ½% Ti. QUENCHED FROM 900°C TO 625°C, HELD ISOTHERMALLY FOR 98HR, WATER QUENCHED. X200

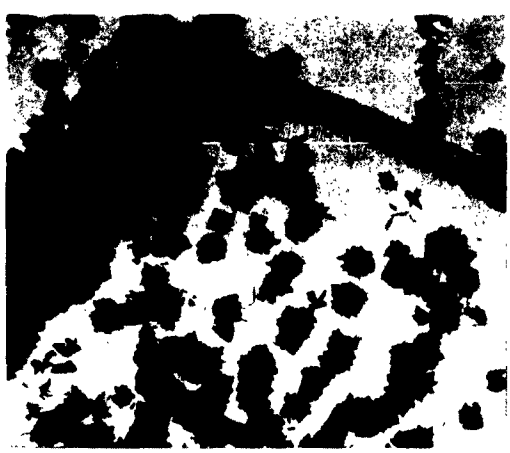

EARLY STAGE
OF TRANSFORMATION

FIG. 28: U - 2% Mo - 2% Nb - 2% Zr - ½% Ti. QUENCHED FROM 900°C TO 550°C, HELD ISOTHERMALLY FOR 30 MIN, WATER QUENCHED. X500

(SEE FIG. 24)

FIG. 29: U-2% Mo-2% Nb-2%V-$\frac{1}{2}$%Ti. SAMPLE E 106-3B. OIL QUENCHED FROM 927°C. X500

(SEE PAGE 28)

FIG. 30: U-8% Mo, SAMPLE E 101-5B. FURNACE COOLED FROM 927°C. X150
CELLULAR REACTION (SEE PAGE 31)

FIG. 31 : U - 8 % Mo. SAMPLE E 101 - 5A WATER QUENCHED FROM 927°C. X100

(SEE PAGE 30)

FIG. 32 : U - 2 % Mo - 2 % Nb - 2 % V - $\frac{1}{2}$ % Ti. SAMPLE E 106 - 2A. FURNACE COOLED FROM 927°C. X500°

(SEE PAGE 31)

FIG. 33: U-2% Mo-2% Nb-2% Zr-½% Ti. SAMPLE E105-3B. WATER QUENCHED FROM 816°C, AGED AT 566°C.

(SEE PAGE 32)

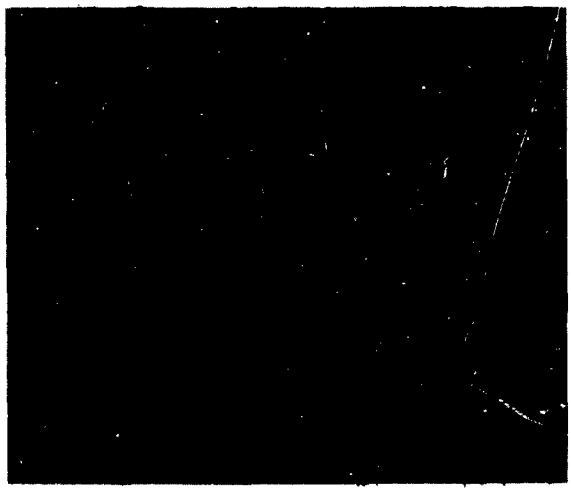

FIG. 34: U-2% Mo-2% Nb-2% Zr-½% Ti. SAMPLE E 105-5B. WATER QUENCHED FROM 816°C, AGED AT 370°C. X500

(SEE PAGE 32)

AD_____ Accession No. _____
U. S. Army Materials Research Agency, Watertown 72, Mass.
TRANSFORMATION CHARACTERISTICS OF THREE URANIUM BASE ALLOYS
P. E. Repas, R. H. Goodenow and R. F. Hehemann
Case Institute of Technology, Cleveland, Ohio

Report No. AMRA CR 63-02/1 (F), January 1 to December 31 1962, 39 pp - tables - illus., (Contract DA-33-019-ORD-3630), D/A Project 5N12-15-030, Unclassified Report

TTT diagrams are presented and transformation kinetics are described for five alloys: (1) U-10%Mo, (2) U-8%Mo, (3) U-8% Mo-1/2%Ti, (4) U-8%Mo-1%Ti, and (5) U-2%Mo-2%Nb-2%Zr-1/2%Ti. Metallographic, dilatometric, hardness and x-ray techniques were utilized in establishing the TTT diagrams. Sensitivity and limitations of each technique are discussed.

UNCLASSIFIED

AD_____ Accession No. _____
U. S. Army Materials Research Agency, Watertown 72, Mass.
TRANSFORMATION CHARACTERISTICS OF THREE URANIUM BASE ALLOYS
P. E. Repas, R. H. Goodenow and R. F. Hehemann
Case Institute of Technology, Cleveland, Ohio

Report No. AMRA CR 63-02/1 (F), January 1 to December 31 1962, 39 pp - tables - illus., (Contract DA-33-019-ORD-3630), D/A Project 5N12-15-030, Unclassified Report

TTT diagrams are presented and transformation kinetics are described for five alloys: (1) U-10%Mo, (2) U-8%Mo, (3) U-8% Mo-1/2%Ti, (4) U-8%Mo-1%Ti, and (5) U-2%Mo-2%Nb-2%Zr-1/2%Ti. Metallographic, dilatometric, hardness and x-ray techniques were utilized in establishing the TTT diagrams. Sensitivity and limitations of each technique are discussed.

UNCLASSIFIED

AD_____ Accession No. _____
U. S. Army Materials Research Agency, Watertown 72, Mass.
TRANSFORMATION CHARACTERISTICS OF THREE URANIUM BASE ALLOYS
P. E. Repas, R. H. Goodenow and R. F. Hehemann
Case Institute of Technology, Cleveland, Ohio

Report No. AMRA CR 63-02/1 (F), January 1 to December 31 1962, 39 pp - tables - illus., (Contract DA-33-019-ORD-3630), D/A Project 5N12-15-030, Unclassified Report

TTT diagrams are presented and transformation kinetics are described for five alloys: (1) U-10%Mo, (2) U-8%Mo, (3) U-8% Mo-1/2%Ti, (4) U-8%Mo-1%Ti, and (5) U-2%Mo-2%Nb-2%Zr-1/2%Ti. Metallographic, dilatometric, hardness and x-ray techniques were utilized in establishing the TTT diagrams. Sensitivity and limitations of each technique are discussed.

UNCLASSIFIED

AD_____ Accession No. _____
U. S. Army Materials Research Agency, Watertown 72, Mass.
TRANSFORMATION CHARACTERISTICS OF THREE URANIUM BASE ALLOYS
P. E. Repas, R. H. Goodenow and R. F. Hehemann
Case Institute of Technology, Cleveland, Ohio

Report No. AMRA CR 63-02/1 (F), January 1 to December 31 1962, 39 pp - tables - illus., (Contract DA-33-019-ORD-3630), D/A Project 5N12-15-030, Unclassified Report

TTT diagrams are presented and transformation kinetics are described for five alloys: (1) U-10%Mo, (2) U-8%Mo, (3) U-8% Mo-1/2%Ti, (4) U-8%Mo-1%Ti, and (5) U-2%Mo-2%Nb-2%Zr-1/2%Ti. Metallographic, dilatometric, hardness and x-ray techniques were utilized in establishing the TTT diagrams. Sensitivity and limitations of each technique are discussed.

UNCLASSIFIED